Free Energetics of NaI Contact and Solvent-Separated Ion Pairs in Water Clusters

Gilles H. Peslherbe,*,†,‡,§ Branka M. Ladanyi,† and James T. Hynes‡

Department of Chemistry, Colorado State University, Fort Collins, Colorado 80523, Department of Chemistry and Biochemistry, University of Colorado, Boulder, Colorado 80309-0215, and Department of Chemistry and Biochemistry, Concordia University, Montréal, Québec, Canada H3G 1M8

Received: October 12, 1999; In Final Form: January 31, 2000

The thermodynamic stability of NaI salt ion pairs in water clusters has been investigated by means of ion pair potential of mean force calculations employing Monte Carlo simulations with model potentials and free energy perturbation theory. In the simulations the ion pair is described by semiempirical valence-bond theory, while the water model potentials employed include the standard liquid-phase TIP4P/OPLS and a polarizable five-site water model that we have developed for cluster simulations. The latter model is parameterized in order to reproduce small cluster experimental data supplemented by ab initio MP2 calculations with a modified 6-31+G** basis (and pseudopotentials for iodine). Simulations with both models yield similar qualitative features for the cluster ion pair potentials of mean force and resulting cluster equilibrium constants, even though they exhibit some quantitative differences. A major finding of our theoretical study is that the ion pair is quite stable with respect to dissociation into free ions, even in very large clusters, and an analysis of cluster solvation energies with a simple dielectric model suggests that the stability of the ion pairs is in fact related to the very slow convergence of cluster ion solvation energies with increasing cluster size, which makes separated cluster ions thermodynamically unlikely. Rather, the ion pairs tend to exist as "contact" ion pairs and solvent-separated ion pairs in the larger clusters, a feature which is likely to be overemphasized in simulations with the TIP4P/OPLS model potentials, which illustrates the importance of solvent−solvent and solute−solvent polarization in model potentials. Preliminary ab initio characterization of model cluster excited states suggests that $NaI(H_2O)_n$ cluster "contact" ion pairs have optically accessible excited states akin to that of gas-phase NaI, hence making photodissociation experiments feasible, but that electronic transition oscillator strengths significantly decrease for model solvent-separated ion pairs. As a result, the larger cluster ion pairs, which are mainly solvent-separated, will not be involved in cluster photodissociation reactions via a mechanism akin to gas-phase NaI photodissociation, in agreement with recent experimental findings.

I. Introduction

There has been a long-standing interest in understanding how the presence of polar solvent molecules affects chemical reactions or the physical and chemical properties of species, and increasing attention is being devoted to investigating microsolvation in clusters as a relatively new avenue in this pursuit.[1,2] A number of ion−solvent[3−13] and pure solvent[14−18] cluster experimental and theoretical studies have been reported, primarily focusing on cluster structures, thermodynamics, and spectroscopy. However, there has been, to our knowledge, very little work reported on the solvation of simple ion pairs or salts in clusters,[19−23] and in this article, we report a theoretical investigation of the thermodynamics of the alkali halide salt NaI in water clusters. Water is evidently a solvent of choice, given its importance.[24]

Further, studies of salts in water clusters should be relevant in environmental chemistry, atmospheric chemistry, and cloud physics. For example, such studies could bring some insight into the formation mechanism of cloud aerosols, which are typically generated in cloud chambers by silver halide vapor seeding[25] or in the atmosphere by spraying silver iodide smokes from aircrafts.[25,26] Such smokes contain mixtures of AgI, NaI, and KI,[26] and have been used to saturate clouds, thus artificially making rain on a large scale.[25−27] A number of recent laboratory studies have focused on the chemistry of various atmospherically relevant compounds on hydrated sea-salt particles[28,29] or on water droplets containing sodium chloride or iodide, and the reaction kinetics were found to differ from that of the bulk for aerosols typically of a few hundred μm.[29] It is thought that the heterogeneous chemistry in concentrated sea-salt aerosols may play an important role in determining the concentration of key compounds such as atomic chlorine in the marine boundary layer.[28,29]

Most relevant to our own current work, the structural and thermodynamic properties of the $NaI(H_2O)_n$ clusters may play an important role in their photodissociation dynamics, as now discussed. The NaI system has become the prototype system for the study of photodissociation dynamics involving curve crossing of covalent and ionic states.[30−36] Briefly, photoexcitation of the ground state NaI to the first excited state results in bound oscillatory motion in the excited state potential, modulated by predissociation to the ground state, the latter arising from the crossing of the diabatic covalent and ionic curves which are electronically coupled.[30] Our own interest in NaI has centered on the photodissociation dynamics for this system in solution[37] and in clusters.[38,39] Our earlier work[37] indicated that radiative deactivation to the ground ionic state would follow

* Corresponding author.
† Colorado State University.
‡ University of Colorado.
§ Condordia University.

10.1021/jp993641t CCC: $19.00
Published on Web 04/21/2000

photoexcitation of the NaI ion pair in a weakly polar solvent, but that more interesting photodissociation dynamics may occur in small clusters. In a first installment of the NaI photodissociation dynamics in clusters,[38] we examined the photodissociation dynamics of the $NaI(H_2O)$ system, focusing particularly on mechanistic aspects and the differences compared to the isolated NaI case. It was found that the clustered water enhances the probability of an excited to ground state nonadiabatic transition, with muted oscillatory dynamics present for the bound excited-state motion. Other important features of the process include a considerable transfer of rotational kinetic energy to the water molecule and a rapid "evaporation" of that molecule. The simulated probe signal for $NaI(H_2O)$ photoionization was found to be in reasonable agreement with the experimental observable.[40]

We are now in the process of studying the photodissociation dynamics of larger $NaI(H_2O)_n$ clusters,[39] in order to make a more thorough connection with ongoing companion experiments.[40] One of the main issues that we addressed in the past is the stability of the ground state ion pair with respect to dissociation in the presence of polar solvent molecules,[37] which is at the heart of the feasibility of the photodissociation experiments (one needs a stable ground state ion pair with an optically accessible excited state to start with). It is well known that salts are fully ionized in aqueous solution, and simple saturation concentration arguments suggest that the NaI ion pair is dissociated in a solution with a H_2O/NaI mole ratio of only 5.[41] Even though it is questionable to compare $NaI(H_2O)_n$ cluster properties to those of saturated NaI aqueous solutions, as there may be significant concentration effects in solution whereas the cluster only contains one NaI solute − hence corresponding to a rather dilute state, one might not expect according to such an argument the $NaI(H_2O)_n$ ion pair cluster to be stable with respect to dissociation over a very wide range of cluster sizes. Yet, the results to be described herein indicate that $NaI(H_2O)_n$ ion pairs are in fact quite stable against complete dissociation to free ions for clusters of significant size. Indeed, recent experiments[42] related to our theoretical work indicate that cluster products of $NaI(H_2O)_n$ photodissociation may contain up to 50 water molecules, suggesting that the parent $NaI(H_2O)_n$ ion pair cluster is stable with respect to ground state dissociation and that its first electronic excited state is optically accessible for cluster sizes as large as $n = 50$, and possibly larger if one takes into account possible water evaporation following cluster photoexcitation.

Some of the main questions that we address in this article are the following: is the ground state NaI ion pair indeed thermodynamically stable with respect to complete dissociation in clusters, in contrast to the bulk? And if so, over what range of cluster sizes and why is it the case? We also pay attention to the availability of optically accessible excited states for the ion pair clusters, and discuss the possible implications of our preliminary findings for the cluster photodissociation dynamics, while we defer a more detailed analysis of other properties of the $NaI(H_2O)_n$ clusters, such as their structure at room temperature, to a later publication.[43]

Monte Carlo simulations are employed to generate canonical ensembles of clusters at room temperature, and the stability of the ion pair is investigated via computations of the ion pair potential of mean force[44] and related equilibrium constants. A number of such simulations have been reported for ion pairs in liquid water,[45−47] but, to our knowledge, very few studies have focused on ion pairs in water clusters.[19−21] The potential of mean force calculations for NaCl salt in liquid water suggest that ion pairs are thermodynamically more likely to exist as solvent-separated ion pairs (SSIP) and even far more likely as "free" ions in solution than as "contact" ion pairs (CIP), confirming (not surprisingly) that salts "ionize" even in infinitely dilute aqueous solutions.[45] The above simulations have employed water model potentials primarily derived for reproducing liquid water properties, but it has been recently recognized that such potentials may not be adequate for studies of clusters, such as pure water clusters,[16] and that new water model potentials may be needed to appropriately describe cluster properties. In the course of this work, we have developed our own water model, a simple polarizable five-site model potential, together with optimized potentials for cluster simulations (OPCS), for describing solute−solvent interactions, which are aimed toward a good description of the gas-phase water properties, ion−solvent and ion pair−solvent complex structures, and binding energies. Cluster simulations are also performed with the well-known TIP4P water potential[48] supplemented with optimized potentials for liquid simulations (OPLS),[49] for comparison.

The outline of the remainder of this article is as follows: we first review in section II the various ingredients of the $NaI(H_2O)_n$ cluster simulations, including the model potentials and the basic theoretical concepts employed. We then present and discuss the simulation results in section III, focusing on the cluster thermodynamic properties, the stability of the ion pair in clusters, and the possible implications for the cluster photodissociation dynamics. Concluding remarks follow in section IV.

II. Simulation Procedure

A. Monte Carlo Simulations. Canonical ensembles of clusters at room temperature are generated as Markov chains by the random-walk Metropolis Monte Carlo method,[50] a technique which has proven more efficient than the molecular dynamics method for equilibrium conformational sampling.[51] In the present simulations, NaI is held fixed in space at a given internuclear separation, and a trial new configuration is generated by randomly translating one water molecule at a time in each Cartesian direction and rotating it about its Euler angles. Because one random walk involves the six degrees of freedom of only one water molecule, the length of the Markov chain used for the statistical averaging involved in the potential of mean force calculations discussed below naturally increases with cluster size. The ranges of displacements were typically chosen as 0.2 Å for translation and 20°, 0.2, and 20° for φ, $\cos\theta$ and ψ, respectively, where φ, θ, and ψ are the standard Euler angles.[50] This prescription ensures an overall acceptance ratio of ∼40% for new configurations. Independent simulations are carried out for a number of cluster sizes.

In contrast to liquid simulations,[50] no potential truncation is necessary and obviously no periodic boundary conditions should be imposed. However, attention must be paid to water evaporation from the clusters (a possible event at room temperature) in order to sample a well-defined equilibrium ensemble of stable clusters of a given size.[52] This is achieved by adding a stepfunction in the configurational integral, so as not to take into account clusters that have undergone one or more water evaporations.[10,53] In practice, the conformational data is collected in chains of 10 000 configurations, and each chain containing clusters that have undergone water evaporation is excluded from the final conformational sampling. We consider a water as evaporated from the cluster when it is farther than 15 to 20 Å from the nearest of the ions, depending on the cluster size. Each simulation entails 10^4 to 5×10^6 configurations of equilibration,

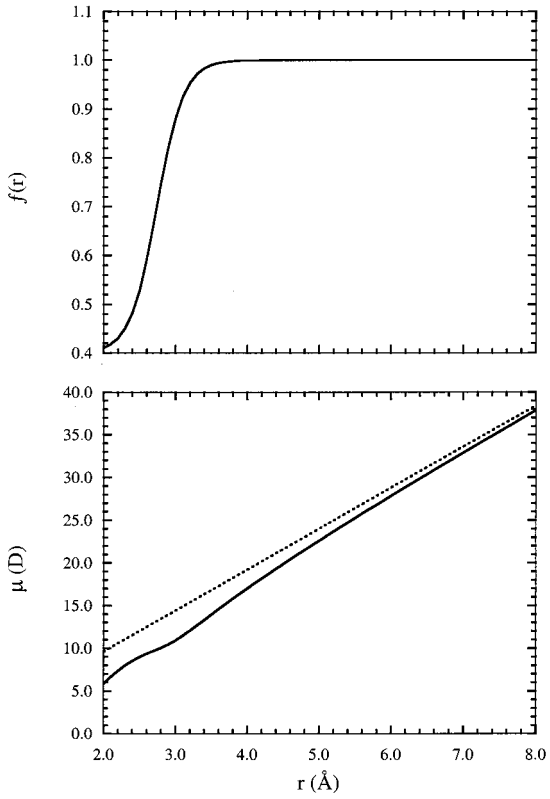

Figure 1. Classical polarizable model for the NaI ion pair. (a) switching function $f(r)$ used in attenuating the ion polarizabilities at small internuclear separations; (b) resulting NaI dipole moment (the dashed line represents the dipole moment of an $Na^{+1}I^{-1}$ ion pair).

followed by an equivalent number of steps of conformational data collecting, depending on the size of the cluster. Finally, to attempt sampling of multiple possible local minima,[54] the clusters are periodically heated and cooled with a smooth temperature schedule.

B. Model Potentials. The potentials used in the cluster simulations consist of NaI solute potentials derived from semiempirical quantum chemistry, classical solvent−solvent and solute−solvent intermolecular potentials.

1. Solute Potentials. The NaI ion pair potential model has been reported in earlier publications,[37,38] to which the reader is referred for details. Briefly, a semiempirical quantum chemistry approach is employed to calculate the energy of Na^+I^- (and other valence-bond structures) as a function of internuclear separation r. Only two electrons are treated explicitly, while the contribution due to the remaining electrons is embedded in a core−core + classical polarization potential, and all electron integrals are evaluated under the point-charge, Pariser and Mulliken approximations,[55] resulting in analytical expressions. The classical polarization part of the model corrects for the shortcomings of the valence-only minimum basis set approach of semiempirical quantum chemistry;[38] in this model, the interaction of the ion polarizability with the other ion unit point charge induces dipole moments which are added to the permanent dipole moment due solely to the ion point charges.

The ion polarizabilities are smoothly attenuated with decreasing internuclear separations, since the effective polarizability of the ions should naturally decline in the presence of other species. A smooth switching function $f(r) = 0.7 + 0.3 \tanh[(r/\text{Å}-2.74)/0.37]$ used for this purpose is displayed in Figure 1. This switching function has been parameterized[38] so that the dipole moments of the ground and first excited states of NaI, calculated via valence-bond theory and our semiempirical quantum chemistry + classical polarization scheme, agree well both with those predicted by high level ab initio calculations[56] and with the experimental value for ground-state NaI at its equilibrium internuclear separation (∼9.2 D).[57] The resulting dipole moment for the isolated NaI ion pair is displayed in Figure 1, where it is also shown that the deviation, the induced dipole contribution, from the dipole moment calculated with unit point charges on the ions is not negligible at short separations. Apparent or effective ion point charges δ can be extracted from the total dipole moment of the ion pair and, for example, δ is 0.75 for $Na^{+\delta}I^{-\delta}$ at the gas-phase equilibrium internuclear separation of ∼2.7 Å.

Finally, the core−core potentials, which are represented by exponentially repulsive walls, were parameterized[38] to reproduce, via valence-bond theory, the relative energies of the ground and first excited states of NaI determined either experimentally[30] or from high level ab initio calculations.[56] The resulting potential energy expression for the NaI ion pair is

$$U_{\text{NaI}}(r) = Ae^{-Br} - \frac{e^2}{r} + U_{\text{pol}}(r) \qquad (1)$$

where $A = 70\,810$ kcal/mol, $B = 0.326$ Å^{-1}, and the energy of the free ions defines the zero of energy. The U_{pol} term in eq 1 is the classical polarization potential due to both the interaction of the aforementioned induced dipoles with the ion unit point charges and the induced dipole−induced dipole interactions. For the isolated NaI ion pair, it is the well-known expression[58]

$$U^0_{\text{pol}}(r) = -\frac{(\alpha_{Na^+} + \alpha_{I^-})e^2}{2r^4} - \frac{2\alpha_{Na^+}\cdot\alpha_{I^-}e^2}{r^7} \qquad (2)$$

where the α's are the ion polarizabilities (which are attenuated by a switching function at short separations). The superscript 0 in eq 2 identifies this as the polarization energy of an isolated NaI, or an ion pair whose polarization is unaffected by the presence of solvent molecules, as will become clear in a moment. Display of the isolated NaI potential energy curve is deferred to Figure 3, where it is shown with the cluster potentials of mean force, for a convenient comparison.

2. Solvent Model Potentials. Of the two water potentials used in the simulations, one is the TIP4P model,[48] which employs a rigid water molecule with experimental gas-phase geometry ($r_{OH} = 0.9572$ Å and $\theta_{H-O-H} = 104.52°$) and four interaction sites centered on the three nuclei and at a fourth (M) on the bisector of the H−O−H angle, 0.15 Å from oxygen toward the hydrogens. The hydrogens and the M site have point charges of $0.52e$ and $-1.04e$, respectively, while the oxygen, bearing no charge, carries a repulsion−dispersion term, i.e., a Lennard-Jones potential term with parameters $\epsilon_{O-O} = 0.155$ kcal/mol and $\sigma_{O-O} = 3.154$ Å. The solute−solvent OPLS parameters for Na^+-H_2O interactions ($\epsilon_{O-Na^+} = 0.499$ kcal/mol and $\sigma_{O-Na^+} = 2.446$ Å) are taken from Jorgensen and co-workers,[49] while the parameters for I^--H_2O interactions ($\epsilon_{O-I^-} = 0.225$ kcal/mol and $\sigma_{O-I^-} = 3.970$ Å), which have not been reported to our knowledge, were derived so as to reproduce the experimental interaction energy and the calculated HF/3-21+G geometry of the ion−water complex, as was done in earlier work for other halide−water interactions.[49] In the present simulations with OPLS, the sodium and iodide ions bear apparent fractional charges extracted from the NaI dipole moments as described above, i.e., the charges are less than unity at short NaI internuclear separations.

Turning to the second water model, there is some legitimate concern, as mentioned earlier, that water model potentials

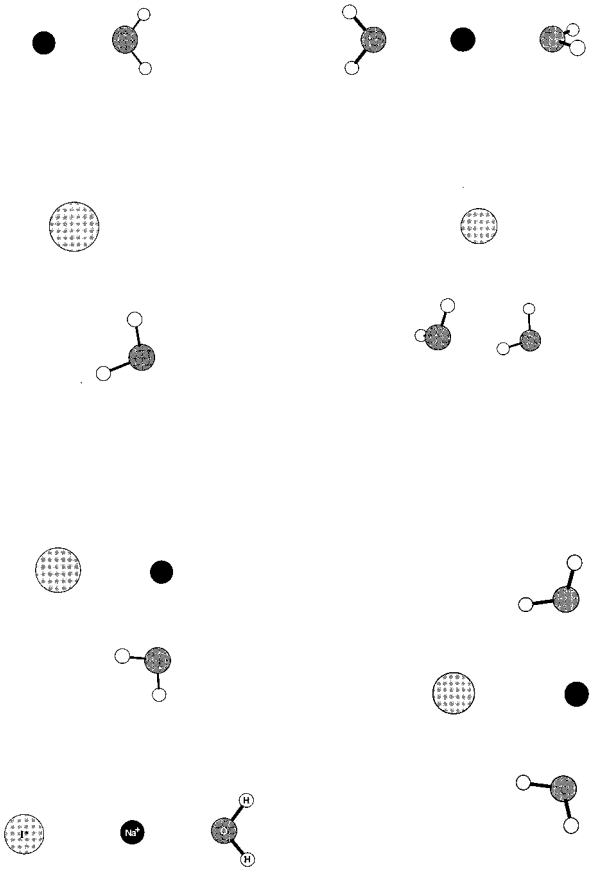

Figure 2. $NaI(H_2O)_n$, $Na^+(H_2O)_n$, and $I^-(H_2O)_n$ cluster minimum energy structures, $n = 1, 2$.

derived to reproduce bulk liquid properties may not be adequate for simulations of small clusters.[16] For example, the TIP4P water dimerization energy is an overestimate of ~20%, since the effective TIP4P potential is parameterized to yield the proper hydrogen bond energy in the bulk, not that in the gas phase.[48] We have developed, initially solely for the purpose of cluster simulations, a simple polarizable five-site water model, together with optimized potentials for cluster simulations (OPCS) for the ion−water interactions. It turns out that our water model also provides a good description of bulk liquid water and details of the model properties will be given elsewhere.[59] Accordingly, we will only outline the main features of the water model here.

Our water model also employs a rigid water molecule with experimental gas-phase geometry, and its functional form is inspired by that of the NEMO water model[60] but it is simplified. The NEMO model consists of four charge sites (one on each water H and two near the water O off the molecular plane), and polarizable and repulsion−dispersion sites on each atom.[60] As outlined below, our model retains the four charge sites approach, but employs only one polarizable and repulsion−dispersion site on the water O (as is customarily done for liquid phase model potentials) and H−H repulsion potential terms. We also depart from the approach[61] used in parameterizing the NEMO model by using as much experimental data as possible. In particular, we take for the basis of parameterization data for isolated species and small clusters. The water−water interactions, and even more so the ion−water interactions, can be viewed as mainly electrostatic, which motivates our decision to include electric moments of water higher than the dipole moment in the model parameterization procedure.[62]

Requiring the water model point charge distribution to have both the exact dipole and quadrupole moments of gas-phase water makes it necessary to use at least four charge sites.[63] Basically, both of the hydrogens carry a charge q_H, while two M sites located on the bisector of the H−O−H angle but off the water plane by an angle $\pm\theta_{H_2O-M}$ carry a charge $-q_H$. It should be noted that the projection of the two M sites on the water plane resembles the M site of the TIP4P water, and, in a sense, our water model is a 3-dimensional generalization of the 2-dimensional TIP4P model with improved moments of the point charge distribution.

To account for nonadditive many-body effects, the oxygen site carries a polarizability, chosen as the experimental isotropic polarizability of the isolated water molecule. The system polarization energy is calculated from[16]

$$U_{\mathrm{pol}} = -\frac{1}{2}\sum_i \mu_i \mathbf{E}_i^0 \tag{3}$$

where the μ_i's are the induced dipoles on the polarizable sites and $\mathbf{E}_i^0$ is the electric field at site i due to the permanent charges of the system q_j:

$$\mathbf{E}_i^0 = \sum_{j\neq i} \frac{q_j \mathbf{r}_{ij}}{r_{ij}^3} \tag{4}$$

The induced dipoles express the response via the polarizability to the total electric field due to the permanent charges and the interactions with other induced dipoles as

$$\mu_i = \alpha_i[\mathbf{E}_i^0 + \sum_{j\neq i} \mathbf{T}_{ij}\cdot\mu_j] \tag{5}$$

where $\mathbf{T}_{ij}$ is the symmetric dipole tensor

$$\mathbf{T}_{ij} = \frac{1}{r_{ij}^3}\left(\frac{3\mathbf{r}_{ij}\mathbf{r}_{ij}}{r_{ij}^2} - \mathbf{I}\right) \tag{6}$$

and $\mathbf{I}$ is the unit tensor. In bulk liquid simulations, eq 5 is usually solved self-consistently by an iterative procedure,[16,64] but in the cluster case, the low dimensionality of the problem allows a straightforward solution of the set of linear equations in matrix form.[65] In the present work, the induced dipoles are solved for by LU decomposition and backsubstitution.[66]

The oxygen site also carries a repulsion−dispersion term as in the TIP4P model, and repulsion terms of the exponential form Ae^{-Br} are added between hydrogens. The intermolecular parameters for these potential terms are chosen to reproduce a wide range of experimental water dimer properties, such as binding energy, geometry, electrostatic properties, and vibrational bending frequency.[59] The resulting parameters are listed in Table 1.

3. Solute−Solvent Potentials. The ion−water interactions are modeled via Coulombic, polarization and Lennard-Jones potentials. The permanent charges on the ions are $\pm 1.0e$ and the polarizabilities of the free ions are naturally chosen as the gas-phase estimates of the ion polarizabilities, which are slightly different from their counterparts measured in crystals[67] (note that, when the ions exist as an ion pair, their polarizabilities are attenuated as discussed in section II.B.1). The ion polarizable sites are included in the induced dipole problem of eqs 3−5, allowing the solvent molecules and the NaI solute to polarize each other, and the polarization energy of NaI is embedded in eq 3 together with eq 1, so that no use is made of eq 2 with the OPCS model (in contrast to simulations with the OPLS model). This is, to our knowledge, the first simulation of an ion pair in

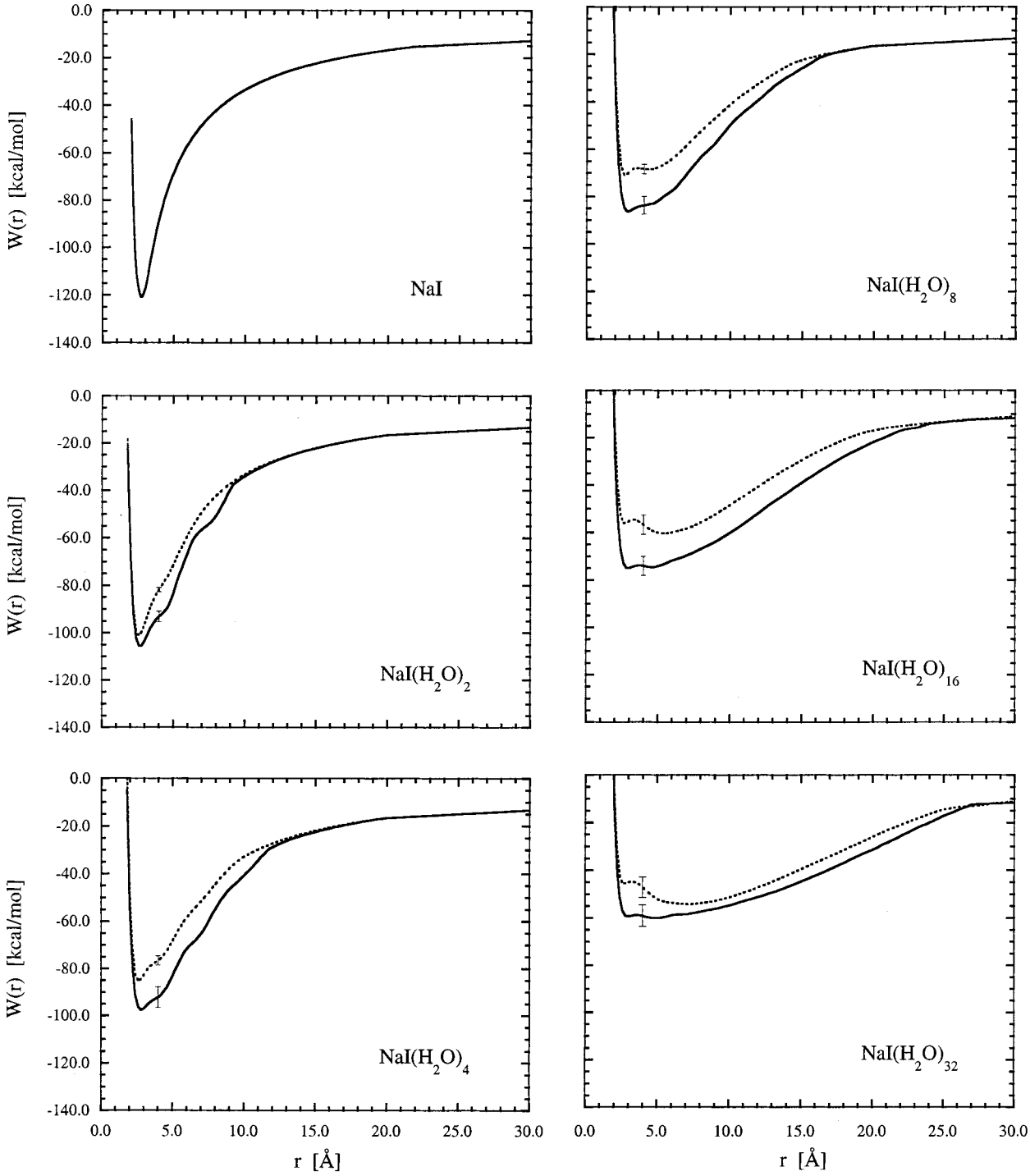

Figure 3. OPLS (dotted line) and OPCS (solid line) potential of mean force results for $NaI(H_2O)_n$ clusters at 300 K.

a polar environment in which polar solvent molecules and solute can polarize each other,[68] although this technique has been used extensively in ion−water simulations.[8b,c] It will be seen that this feature has important consequences.

Once the Coulombic and polarization parts of the solute−solvent interaction potentials have been properly parameterized, the remaining model potential parameters are those of the Lennard-Jones terms, which are adjusted to fit experimental ion−water binding energies and the ion−water complex ab initio minimum energy structure geometries (which are shown in Figure 2). The parameters are listed in Table 1, and the ion−water and small $NaI(H_2O)_n$ cluster properties calculated with the OPCS model are given in Table 2, where they are compared to the properties predicted by the OPLS model and ab initio calculations, and to experimental numbers when available.

The ab initio calculations just referred to were performed with the quantum chemistry packages *Gamess*[69] and *Gaussian 98*.[70] Ground state equilibrium geometries and energies of small ion−water and ion pair−water clusters were computed at the MP2 level[71] with a modified 6-31+G** basis set.[72] Relativistic Stevens/Basch/Krauss/Jasien/Cundari[73] (SBK) effective core potentials are employed for the iodine core electrons, while the iodine valence basis consists of SBK double-split (−41) basis functions, polarization functions, and diffuse functions (with exponent 0.0368). We use a standard 6-31G* basis[72] for sodium, and a 6-31+G(2d,p) basis[72,74] for water. It was recognized

TABLE 1: Model Potential Parameters[a]

Water		
$R_{O-H} = 0.9572$ Å[b]		$\theta_{H-O-H} = 104.52°$[b]
$R_{O-M} = 0.342$ Å	$\theta_{H_2O-M} = 43.4°$	$q_H/e = 0.569$
	$\alpha_W = 1.45$ Å^3[c]	
$\epsilon_{O-O} = 0.25$ kcal/mol		$\sigma_{O-O} = 3.20$ Å
$A_{H-H} = 10^5$ kcal/mol		$B_{H-H} = 5.5$ Å^{-1}
Na^+		
$q_{Na^+}/e = 1.0$		$\alpha_{Na^+} = 0.2$ Å^3[d]
$\epsilon_{O-Na^+} = 0.042$ kcal/mol		$\sigma_{O-Na^+} = 3.11$ Å
I^-		
$q_{I^-}/e = 1.0$		$\alpha_{I^-} = 7.0$ Å^3[d]
$\epsilon_{O-I^-} = 0.85$ kcal/mol		$\alpha_{O-I^-} = 3.81$ Å

[a] Parameters are described in the text. They are either taken from experiment (when indicated) or obtained by fitting the data in Table 2. [b] From Benedict, W. S.; Gailar, N.; Plyler, E. K. *J. Chem. Phys.* **1956**, *24*, 1139. [c] Isotropic water polarizability from *CRC Handbook of Chemistry and Physics*, 77th Edition; Lide, D. R., Ed.; CRC: Boca Raton, FL, 1996. [d] Average gas-phase polarizabilities of the ions from Tessman, J. R.; Kahn, A. H.; Shockley, W. *Phys. Rev.* **1953**, 92, 890.

early[75] that, in order to reproduce the water electrostatic properties with a double-ζ-quality basis set, one needs to add at least two sets of "standard" polarization functions or one set with a smaller-than-usual exponent for the oxygen atom basis. Because we believe the interactions between ions and water in clusters can be viewed as mainly electrostatic, we chose to add a second set of polarization functions to the water basis, which greatly assists in reproducing the water gas-phase dipole moment (1.85 D)[41] at the MP2 level of theory. To summarize, our basis set is a modified 6-31+G** basis, with pseudopotentials for iodine, an additional set of polarization functions for oxygen, and no diffuse functions on sodium. This basis is of reasonable size, and MP2 calculations with such double-ζ-quality valence basis sets usually yield reliable ground-state geometries, energies, and electrostatic properties.[71] We note in passing that this level of theory is an improvement over the ab initio calculations, typically HF/3-21G, employed in previous parameterizations of ion−water interaction potentials.[49]

The cluster geometries were first optimized with the water molecules fixed at their gas-phase geometry, and then were fully optimized in order to evaluate vibrational frequencies. The effect of water geometry relaxation was found to be negligible, resulting in bond length and energy changes usually less than 0.01 Å and 0.2 kcal/mol, respectively. Cluster binding energies were then evaluated and corrected for basis set superposition error (BSSE)[71] estimated by the counterpoise method[76] and for zero-point energy differences. Effective atomic point charges were extracted from the cluster electronic wave function by fitting the electrostatic potential over a large grid of points,[77] and the water dipole moments were simply calculated from this resulting ESP point-charge description. It is seen in Table 2 that our ab initio calculations reproduce the experimental cluster binding energies within quantum chemical accuracy, which inspires some confidence in the overall level of ab initio quantum chemistry selected here.

As mentioned earlier, the ion−water interaction parameters were fitted to reproduce $Na^+(H_2O)$ and $I^-(H_2O)$ cluster properties. Even though they were not included in the parameterization scheme, some properties of the small ion−water clusters (with two waters) and those of the small $NaI(H_2O)_n$ clusters (n = 1−2) predicted by the OPCS model and shown in Table 2 compare favorably to their ab initio or experimental counterparts. The small cluster properties are also reasonably well described by the OPLS model, but as expected, the agreement with ab initio and experimental properties is not as thorough. A notable advantage of the polarizable OPCS model lies in the better description of the charge distribution of the clusters, especially that of the water molecules. For example, the presence of a small charge-concentrated ion such as Na^+ strongly polarizes a nearby water molecule and enhances its dipole moment (see Table 2),

TABLE 2: Ion−Water and $NaI(H_2O)_n$ Cluster Properties[a]

	model potentials			
	OPLS	OPCS	expt.	ab initio
NaI				
R_{NaI}		2.7	2.71[b]	2.76
μ_{NaI}		9.7	9.2[c]	9.7
D_0		120.7	116.6[b]	115.8
H_2O				
μ_{H_2O}	2.2	1.85	1.85[d]	2.0
$Na^+(H_2O)$				
q_{Na^+}/e	1.0	1.0		1.0
μ_{H_2O}	2.2	3.2		2.9
R_{O-Na^+}	2.24	2.28		2.27
$\theta(\mu_{H_2O},\mathbf{R}_{O-Na^+})$	180	180		180
D_0	24.1	24.6	24.0[e]	21.1
$I^-(H_2O)$				
q_{I^-}/e	−1.0	−1.0		−0.96
μ_{H_2O}	2.2	2.3		2.4
R_{O-I^-}	3.59	3.69		3.63
$\theta(\mu_{H_2O}, \mathbf{R}_{O-I^-})$	33	42		37
D_0	10.3	10.6	10.3[f]	8.9
$Na^{+\delta}I^{-\delta}(H_2O)$ C_{2v}				
μ_{NaI}	10.0	10.1		9.5
μ_{H_2O}	2.2	2.7		2.1
R_{NaI}	2.74	2.76		2.79
R_{O-Na^+}	2.31	2.36		2.36
R_{O-I^-}	5.05	5.10		5.15
D_0	13.5	16.1		12.9
$Na^{+\delta}I^{-\delta}(H_2O)$				
μ_{NaI}	9.9	10.2		9.8
μ_{H_2O}	2.2	2.5		2.1
R_{NaI}	2.76	2.83		2.84
R_{O-Na^+}	2.31	2.34		2.31
R_{O-I^-}	3.75	3.64		3.50
D_0	14.4	18.0		14.9
$Na^+(H_2O)_2$				
q_{Na^+}/e	1.0	1.0		1.0
μ_{H_2O}	2.2	3.1		3.1
R_{O-Na^+}	2.25	2.31		2.30
D_0	47.0	46.2	44.0[e]	41.2
$I^-(H_2O)_2$				
q_{I^-}/e	−1.0	−1.0		−1.0
μ_{H_2O}	2.2	2.3, 2.3		2.2, 2.7
R_{O-I^-}	3.56, 3.69	3.66, 3.78		3.55, 3.83
D_0	23.0	23.0	19.8[f]	17.5
$Na^{+\delta}I^{-\delta}(H_2O)_2$				
μ_{NaI}	10.2	10.8		10.6
μ_{H_2O}	2.2	2.4		2.1
R_{NaI}	2.83	2.94		2.94
R_{O-Na^+}	2.33	2.35		2.33
R_{O-I^-}	3.71	3.65		3.52
D_0	28.3	34.9		30.1

[a] Cluster binding energies in kcal/mol, bond lengths in Å, dipole moments in D, angles in degrees. Cluster structures are shown in Figure 2. The ab initio results were obtained at the MP2 level of theory with a modified 6-31+G** basis. See text for details. [b] Taken from Varshni, Y. P.; Shukla, R. C. *J. Mol. Spectr.* **1965**, *16*, 63 and references therein. [c] From Hebert, A. J.; Lovas, F. J.; Melenders, C. A.;Hollowell, C. D.;Story, T. L.; Street, K. *J. Chem. Phys.* **1968**, *48*, 2834. [d] From Clough, S. A.; Beers, Y.; Klein, G. P.; Rothman, L. S. *J. Chem. Phys.* **1973**, *59*, 2254. [e] Cluster binding enthalpy at 300 K from Dzidic, I.; Kebarle, P. *J. Phys. Chem.* **1970**, *74*, 1466. Kebarle, P. *Ann. Rev. Phys. Chem.* **1977**, *28*, 445. [f] Cluster binding enthalpy at 300 K from Hiraoka, K.; Mizuse, S.; Yamabe, S. *J. Phys. Chem.* **1988**, *92*, 3943.

a feature that is correctly accounted for by the OPCS model, but that cannot be properly described by the nonpolarizable OPLS model. The respective merits of the OPCS and OPLS models for describing small cluster structures will be discussed elsewhere.[43]

C. Potential of Mean Force and Equilibrium Constants

Finally, the free energetics of the NaI in clusters can be characterized via the potential of mean force $W(r)$ for an ion pair, which describes the free energy or solvent-averaged energy change as the internuclear distance between the ions r is varied.[44] The potential of mean force can be calculated by a variety of techniques such as integral equation techniques,[78] constrained molecular dynamics (MD) methods,[47] and statistical perturbation theory evaluation of free energy differences.[79] We chose the latter route, since the evaluation of free energy differences can naturally be performed in the course of our Monte Carlo equilibrium simulations by symmetrically stretching the ion pair by a distance dr and calculating the system potential energy difference $\Delta U(r) = U(r + dr) - U(r)$. The corresponding free energy or potential of mean force change is then

$$\Delta W(r) = W(r + dr) - W(r) = -kT \ln\langle e^{-\Delta U(r)/kT}\rangle_r = -kT \ln \langle e^{-[U(r+dr)-U(r)]/kT}\rangle_r \quad (7a)$$

$$= -kT \ln\langle e^{-\Delta U(r)/kT}\rangle_{r+dr} = -kT \ln\langle e^{-[U(r+dr)-U(r)]/kT}\rangle_{r+dr} \quad (7b)$$

where $\langle\cdots\rangle$ denotes the canonical ensemble average, and the subscript labels the ensemble considered for averaging and refers to the ion pair internuclear separation at which the simulation is performed. In practice, we use a double-wide sampling of potential energy differences and calculate the equilibrium ensemble average by the acceptance ratio method of Bennett.[80] For every internuclear separation r, we make use of the results of two simulations, one performed with the ion pair at internuclear separation r, and making use of a forward perturbation, we collect the $\Delta U(r) = U(r + dr) - U(r)$ data, and a second simulation performed with the ion pair at internuclear separation $r + dr$, and making use of a backward perturbation, we also collect the $\Delta U(r) = U(r + dr) - U(r)$ data. This provides two independent estimates of the ensemble average in eqs 7, and the final $\Delta W(r)$ is calculated so as to minimize the variance of the ensemble averages.[80] The simple mean of both estimates of the ensemble averages has also been used in previous work[81] as the final ensemble average value, and in many instances, we found that both methods yield very similar potential of mean force differences. Interestingly enough, the hysteresis between the forward and backward perturbation results can be used to estimate the statistical uncertainty in the calculated free energy differences.[81]

The long-range part of the potential of mean force can be represented by a simple Coulombic interaction term between two oppositely charged cluster ions. In practice, we typically carry out cluster simulations from $r = 2$ Å up to $r = 15-30$ Å depending on the cluster size, with a perturbation step size 0.2 Å, add up $\Delta W(r)$ free energy differences (and their statistical uncertainties), and anchor the potential of mean force to a $-e^2/r$ Coulombic potential term in the 15−30 Å range of NaI internuclear separations. In liquid-phase calculations of potentials of mean force, the corresponding limiting value is $-e^2/(\epsilon r)$, where ϵ is the dielectric constant of the solvent in question, but this is not appropriate in clusters, since, at large-enough solute internuclear separations, the potential of mean force represents the potential of two separate cluster ions in a vacuum.

The probability of finding the ions at an internuclear distance r is $4\pi r^2 e^{-W(r)/kT}$ and the equilibrium "contact" ion pair (CIP) population is defined by

$$\langle n_{CIP}\rangle = \frac{4\pi}{V}\int_{CIP} r^2 e^{-W(r)/kT}\, dr \quad (8)$$

where V is the system volume, and the integral runs over internuclear separations representative of the CIP. In contrast to liquid simulations of ion pairs, the volume (or pressure) in clusters is not well defined, but this does not turn out to be problematic in the present analysis, since, as we shall see presently, the volume V cancels out in the expressions for the equilibrium constants of interest.

The CIP dissociation constant is then expressed as[82]

$$\frac{1}{K_{diss}} = \frac{[Na^+I^-]}{[Na^+][I^-]} = 4\pi N_A \int_{CIP} r^2 e^{-W(r)/kT}\, dr \quad (9)$$

where N_A is Avogadro's number and the ion pair and ion concentrations naturally refer to solvated species in clusters.[83] In practice, the integration limits are varied until the dissociation constant is numerically locally converged. In cases where a stable solvent-separated ion pair (SSIP) exists, the position of the CIP to SSIP free energy barrier naturally determines the upper bound of the integral. Finally, the equilibrium constant between the CIP and the SSIP is just[47]

$$K_{eq} = \frac{[SSIP]}{[CIP]} = \frac{\int_{SSIP} r^2 e^{-W(r)/kT}\, dr}{\int_{CIP} r^2 e^{-W(r)/kT}\, dr} \quad (10)$$

where the denominator is just evaluated as for eq 9. The lower bound of the numerator integral is naturally the location of the free energy barrier between the CIP and the SSIP (i.e., the upper bound of the denominator integral). The upper bound for the numerator is varied until the equilibrium constant is locally converged,[84] but it is assigned an upper limit corresponding to the average CIP cluster diameter.[85] The latter choice represents a situation where both ions would have moved apart onto opposite sides of the solvent cluster. Both K_{diss} and K_{eq} will be useful in the characterization of the NaI cluster ion pairs.

III. Ion Pair Cluster Thermodynamics

A. Potentials of Mean Force. The potentials of mean force (pmf) for a variety of cluster sizes are displayed in Figure 3 for both OPLS and OPCS. The main pmf feature for both models is that the well for the ion pair at short internuclear separations is very deep, so that the resulting contact ion pair (CIP) dissociation constants K_{diss} listed in Table 3 are extremely small, indicating the indubitable thermodynamic stability of the ion pairs in clusters. With both models, the pmf well depth decreases with increasing cluster size, which is consistent with the bulk limit (recall that the pmf well depth for alkali halide such as NaCl ion pairs is only a few kcal/mol).[45,86] Figure 3 also shows that for cluster sizes larger than $n = 8$, a second minimum in the pmf emerges, signaling the appearance of a locally stable solvent-separated ion pair (SSIP) species. The details of the stability of the SSIP compared to the CIP evidently depend on the model potentials, and we will return to this below.

TABLE 3: Properties of the Potentials of Mean Force

n	r_{min}^{CIP} [b]	$r^{\ddagger}$ [c]	r_{min}^{SSIP} [d]	$\Delta G^{\ddagger}$ [e]		log K_{diss} [f]	K_{eq} [g]	$d_{cluster}$ [f]
				OPLS − T=300 K				
2	2.6					-71 ± 1		
4	2.6					-60 ± 2		
8	2.7	3.5	4.4	2.8 ± 0.2	0.5 ± 0.2	-50 ± 2	0.2−0.4	10.4
16	2.7	3.3	5.4	1.6 ± 0.1	5.8 ± 0.4	-39 ± 3	$\sim 10^4$	13.4
32	2.7	3.2	7.2	0.8 ± 0.2	9.5 ± 0.8	-31 ± 3	$\sim 10^8$	16.0
				OPCS − T=300 K				
2	2.7					-75 ± 2		
4	2.8					-69 ± 3		
8	2.9					-61 ± 3		
16	2.9	3.7	4.6	1.3 ± 0.1	0.8 ± 0.1	-53 ± 3	2−4	13.2
32	3.0	3.7	4.8	0.6 ± 0.2	1.3 ± 0.5	-42 ± 4	6−70	15.4
				OPCS − T=200 K				
8	2.9					-106 ± 5		
16	3.0	3.7	4.7	0.7 ± 0.3	1.1 ± 0.5	-84 ± 7	2−27	11.8
32	3.1	3.8	4.7	0.6 ± 0.2	0.6 ± 0.6	-74 ± 7	1−50	13.9

[a] Free energies in kcal/mol and distances in Å. [b] NaI internuclear separation of the minimum in the CIP well. [b] NaI internuclear separation of the minimum in the SSIP well. [d] NaI internuclear separation at the CIP to SSIP barrier. [e] Free energy barrier height measured from the minimum in the CIP and from that in the SSIP, respectively. [f] Dissociation constant for the CIP, eq 9, in $(mol/l)^{-1}$. [g] CIP ⇌ SSIP equilibrium constant, eq 10. The range of equilibrium constants is determined by propagating the statistical errors in the free energies in a systematic fashion.

Independently of these details, it is clear that the SSIP is also very stable against complete dissociation to free ions.

In all of the simulations reported here, the maximum statistical uncertainty in the stepwise free energy differences varies from 0.1 to 0.4 kcal/mol for clusters of size 2 to 32, while the corresponding average uncertainties range only from 0.02 to 0.08 kcal/mol. The latter uncertainties, when summed together along the pmf, add up to seemingly large numbers for the absolute pmf well depths, as shown in Figure 3, but one should keep in mind that the statistical uncertainties in the free energy profile itself are rather small (typically, the relative error in the stepwise free energy differences is ∼3%). However, as we shall see presently, small fluctuations in the free energy profiles and associated barriers lead to rather large error bars on the associated equilibrium constants. We note in passing that the efficient Monte Carlo sampling of configurations that results from periodically heating and cooling the clusters greatly assists in obtaining statistical perturbation theory results with small uncertainties.

The most striking global difference between the results for the two model potentials is that, for any cluster size, the depth of the pmf well region (both at the CIP location and throughout any SSIP region) is greater for OPCS than for OPLS. Focusing on the CIP and deferring for the moment the discussion of the relative CIP/SSIP stability, this larger well depth arises from the polarization term in OPCS (cf. section II.B) absent in OPLS.[87] While in both model descriptions water molecules stabilize the free ions more than the CIP, the OPCS polarization term reduces this differential solvation magnitude compared to OPLS, in favor of the ion pair. For example, the average dipole moment of water in $NaI(H_2O)_{32}$ clusters is 2.6 D, while it is only 2.4 and 2.5 D for $I^-(H_2O)_{20}$ and $Na^+(H_2O)_{20}$ clusters, respectively;[43] thus here and in general there is an extra stabilization, due to the polarization, of the CIP *vis a vis* that of the free ions compared to the OPLS situation where the water molecule dipole moment is fixed in magnitude.

B. Relative Stability of the CIP and SSIP. Not only do OPCS predict larger potential of mean force well depths in general, but they also predict CIPs and SSIPs for the larger clusters that are very close in free energy and separated by much smaller barriers than do OPLS, as can be seen from Figure 3 and Table 3. This discrepancy between the model predictions can be traced back, once again, to the polarizable features of

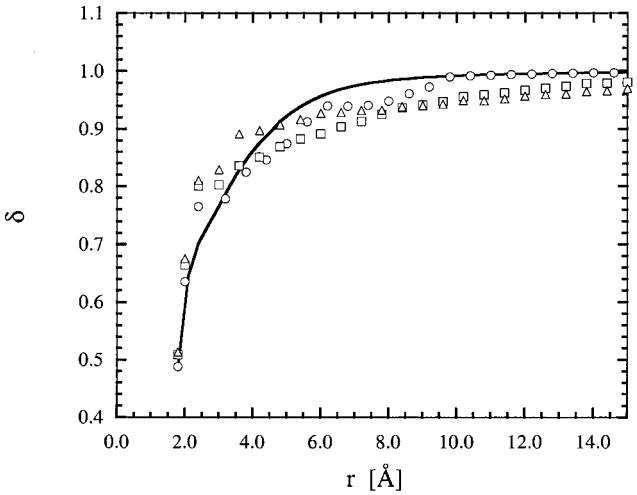

Figure 4. Average effective charge δ in the simulations of $Na^{+\delta}I^{-\delta}(H_2O)_n$ clusters with the OPCS model, for $n = 2$ (○); $n = 8$ (□); and $n = 16$ (△). The solid thick line represents the isolated NaI effective charge used in the simulations with the OPLS model.

OPCS, but this time it is due to the fact that the NaI solute can be polarized by the local solvent environment. As shown in Figure 4, the effective charge δ of $Na^{+\delta}I^{-\delta}$ in the OPCS simulations, i.e., the point charges extracted from the total (permanent + induced) solute dipole moments, are larger than the isolated molecule values at small internuclear separations r, but then tend to converge to unity more slowly than their isolated molecule counterparts (which are used in the OPLS simulations). As a result of this crossover, obvious in Figure 4, the OPCS polarization energy is relatively larger at the smaller internuclear separations, so that the CIP is relatively lower in free energy with OPCS than it is with OPLS. Coincidentally, the CIP is predicted by OPCS to be very close in free energy to the SSIP (while it is higher in energy with OPLS). Note that this by no means indicates that both types of ion pairs are thermodynamically equally probable, as the CIP ⇌ SSIP equilibrium constant expression contains an r-dependent term and the integration limits in eq 10 depend on the location of the free energy barrier between the CIP and the SSIP and the upper bound of the SSIP population integral [i.e., the numerator of eq 10], as discussed in section II.C.

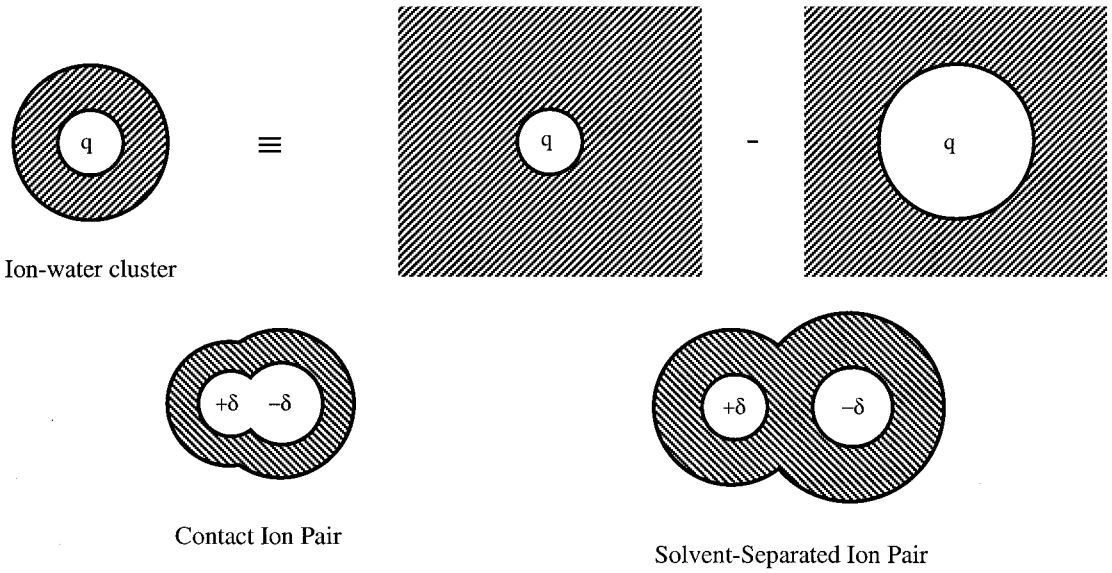

Figure 5. Schematic description of the finite-size dielectric solvation model for ion−water clusters, the contact ion pair and the solvent-separated ion pair.

The free energy barriers between the CIP and SSIP, which are listed in Table 3 for the relevant clusters, are smaller for OPCS than for OPLS, and OPCS predict similar free energetics for both SSIPs and CIPs, while OPLS predict SSIPs significantly lower in free energy than the corresponding CIPs. With both model potentials, the SSIP seems to extend over wider ranges of NaI internuclear separations with cluster size increase, as can be seen in Figure 3 and Table 3. We note in passing that converged equilibrium constants are obtained with upper bounds for the SSIP population integral varying from 6 to 9 Å with increasing cluster size (which are much less than the average CIP cluster diameters listed in Table 3).[85] As a result, cluster ion pairs with internuclear distances exceeding the aforementioned values for the SSIP upper bound do not contribute significantly to the SSIP cluster population, and extreme situations where the ions would be separated by the whole solvent cluster are not representative of SSIP structures.[43]

The equilibrium constants K_{eq}, eq 10, for the CIP ⇌ SSIP listed in Table 3 clearly indicate that, of the two, the SSIP is thermodynamically favored at room temperature for larger clusters, but to an extent which is extremely sensitive to the model potential employed. OPCS predict a SSIP/CIP relative population within about 1 order of magnitude at room temperature, while OPLS predict an overwhelmingly higher stability of the SSIP for clusters of size 16 or larger. In contrast to the bulk behavior, it should be noted that the SSIP in large clusters itself is extremely stable with respect to dissociation, as one can immediately realize from the data listed in Table 3 that the SSIP dissociation constant, given by K_{diss}/K_{eq} is extremely small (as a matter of fact, it is even smaller than the dissociation constant for the CIP). One may wonder at this stage why the ion pairs are so stable with respect to dissociation into free cluster ions, in contrast to the bulk solution problem. We now turn our attention to the origin of this marked ion pair stability.

C. Origin of the Stability of the Ion Pairs with Respect to Dissociation. To help understand ion pair stability issues and cluster solvation effects in general, we employ a simple finite-size continuum dielectric model, first used in applications of the liquid drop model[25,88] to nucleation problems,[89] and recently applied in other studies of cluster solvation.[5,90,91] We have recently reviewed the range of applicability of the liquid drop model and found[92] that, when compared to experimental data or computer simulations results, the continuum dielectric model predicts solvation free energies that are in general surprisingly quite reliable for clusters of all sizes and even shapes (whether the clusters exhibit surface or interior structures).

We first employ a numerical scheme to compute cluster solvation free energies for CIPs and SSIPs as schematically depicted in Figure 5. In this scheme, solvation free (or electrostatic) energies are calculated for ions in spherical cavities carved in a polarizable, dielectric continuum[93] and include solute boundary conditions or dielectric image effects, as used in previous work.[37] We basically compute the approximate cluster solvation free energy by subtracting from the bulk solvation free energy the contribution due to the solvent outside of the cluster cavity.[94] The resulting $NaI(H_2O)_n$ cluster solvation free energies are listed in Table 4 for ions, CIPs, and SSIPs with various arbitrary numbers of water molecules on each ion; the differential solvation free energies are added to the isolated NaI potential gap to obtain the free energy well depths of the model CIPs and SSIPs. The CIP is deeper in free energy than the SSIP for the small clusters, but they become almost iso-energetic with cluster size increase, as was observed in Monte Carlo simulations with OPCS. What is striking about the solvation free energy well depths of the ion pairs listed in Table 4 is that the numbers remain large even for clusters containing several thousands of water molecules, indicating the stability of ion pairs with respect to complete dissociation into free ions in extremely large clusters, in contrast to the bulk solution problem. One may immediately note from inspection of Table 4 that the main reason for the slow convergence to bulk behavior of the potential of mean force well depths is the very slow convergence of the cluster ion solvation free energies to their bulk counterpart, in contrast to the cluster solvation free energies of ion pairs. It is this differential effect that is responsible for the stability of ion pairs in clusters.

The conclusion just reached can be examined in another way. Due to the very long-range nature of ion−solvent interactions, the ion solvation free energies are indeed very slow to converge to the bulk limit.[92] For example, in the liquid drop model,[88] the solvation free energy of an ion (point charge) in a cluster is given by

TABLE 4: Predictions of the Finite-Size Dielectric Solvation Model for the Stability of $NaI(H_2O)_n$[a]

$n = k + l$	k	ΔG_{solv} $Na^+(H_2O)_k$	l	ΔG_{solv} $I^-(H_2O)_l$	ΔG_{solv} CIP[b]	$\Delta G_{CIP/Ions}$[c]	ΔG_{solv} SSIP[d]	$\Delta G_{SSIP/Iins}$[c]
4	2	−36	2	−9	−23	−96	−46	−59
4	3	−42	1	−5	−23	−94	−45	−56
8	4	−47	4	−14	−31	−88	−68	−65
8	5	−50	3	−12	−31	−87	−67	−63
8	6	−52	2	−9	−29	−86	−61	−58
16	8	−56	8	−20	−35	−77	−77	−59
16	9	−58	7	−19	−35	−76	−77	−58
16	10	−59	6	−18	−35	−76	−77	−58
16	11	−60	5	−16	−34	−76	−76	−58
16	12	−61	4	−14	−34	−77	−73	−56
32	16	−64	16	−27	−38	−65	−87	−54
32	17	−65	15	−26	−38	−65	−87	−54
32	18	−65	14	−25	−37	−65	−87	−55
32	19	−66	13	−25	−37	−64	−87	−54
32	20	−67	12	−24	−37	−64	−87	−54
500	225	−84	275	−46	−41	−29	−99	−27
500	250	−84	250	−45	−41	−30	−99	−28
500	275	−85	225	−45	−41	−29	−99	−27
2000	900	−89	1100	−50	−41	−20	−100	−19
2000	1000	−89	1000	−50	−41	−20	−100	−19
2000	1100	−89	900	−50	−41	−20	−100	−19
∞	∞	−98	∞	−59	−41	−2	−101	−2

[a] Free energies in kcal/mol. [b] The contact ion pair (CIP) model used here is $(H_2O)_kNa^{+\delta}I^{-\delta}(H_2O)_l$ with $\delta = 0.9$ and $r = 2.9$ Å. The isolated NaI potential energy is −118 kcal/mol for this internuclear separation. See text for details. [c] Free energy gap between the ion pair cluster and the asymptotic dissociation product clusters. [d] The solvent-separated ion pair (SSIP) model used here is $(H_2O)_kNa^{+\delta}I^{-\delta}(H_2O)_l$ with $\delta = 1.0$ and $r = 5.8$ Å. The isolated NaI potential energy is −58 kcal/mol for this internuclear separation. See text for details.

$$\Delta G_{solv} = -\frac{q^2}{2a}\left(1 - \frac{1}{\epsilon}\right)[1 - a/R] \tag{11}$$

where ϵ is the solvent dielectric constant, and q and a are the ion charge and radius, respectively. The cluster radius R is related to the cluster size by

$$n = \frac{4\pi}{3}(R^3 - a^3)\frac{\rho N_A}{M} \tag{12}$$

where N_A is Avogadro's number, M and ρ are the molecular weight and bulk density of the solvent, respectively. As shown in Figure 6, the model ion−water cluster solvation free energies are very slow to converge to the bulk limit.[92]

On the other hand, the solvation free energy of a dipolar solute in a cluster is approximately[94−96]

$$\Delta G_{solv} = \frac{\epsilon - 1}{8\pi}\int \mathbf{E}\cdot\mathbf{E}_0\, d\mathbf{r} \cong \frac{\epsilon - 1}{8\pi}\frac{3}{2\epsilon + 1}\int \mathbf{E}_0\cdot\mathbf{E}_0 d\mathbf{r} \tag{13}$$

where $\mathbf{E}_0$ is the vacuum solute electric field and the integral is evaluated over the solvent dielectric volume. Evaluation of the latter integral for a point dipole μ in a cavity of radius a embedded in a spherical solvent cluster of radius R yields[95]

$$\Delta G_{solv} = -\frac{\mu^2}{a^3}\frac{\epsilon - 1}{2\epsilon + 1}[1 - (a/R)^3] \tag{14}$$

It is obvious from inspection of Figure 6 and eq 14 that the solvation of ion pairs in clusters converges very fast to the bulk limit (as $1/R^3$), while ion solvation is very slow to reach the bulk limit (as $1/R$). This is responsible for the very slow convergence of the potential of mean force well depth to its (shallow) bulk counterpart, and thus, in other words, for the initially surprising stability of ion pairs with respect to complete dissociation even in large clusters.

Basically, in the cluster case, the large internuclear separation limit corresponds to two oppositely charged clusters in a vacuum; the cluster−cluster attraction energy is then $-e^2/r$. In the bulk case, the two ions at large r are in the same bulk phase, so their attraction is smaller by a factor $1/\epsilon$. This simply explains why the ions attract each other and tend to remain as an ion pair in clusters, in contrast to the bulk problem.

D. Temperature Dependence of the Stability of the CIP and SSIP. The temperature of the clusters in typical $NaI(H_2O)_n$ cluster photodissociation experiments[40] can be estimated to be about 200 K by using the simple renormalized Trouton's rule of the Klots evaporative ensemble model.[97] However, a more refined treatment of ionic clusters within the evaporative ensemble model, using methods for estimating the time-dependent cluster populations and energy distributions which are approximate but quite robust with respect to the empirical parameters employed, indicates that clusters of different sizes have different internal temperatures, and the cluster temperature of some small clusters has been reported to be larger by as much as a factor of 4 compared to that of the larger clusters.[11a] Evidently, there is a wide uncertainty in the estimated cluster temperature of the $NaI(H_2O)_n$ cluster photodissociation experiments.

In this work, we have performed classical Monte Carlo simulations of the clusters at 300 K, as recent studies of ion−water clusters have shown that the quantum effects not addressed here are negligible at room temperature, but become increasingly important as temperature is lowered.[13] Certainly, a large number of classical simulations of clusters have been reported at much lower temperatures typical of cluster molecular beam experiments. We have, however, proceeded in a consistent fashion by first investigating room-temperature clusters with classical simulation techniques.[98] Nevertheless, for the exclusive purpose of perspective, we have also carried out classical simulations at 200 K, a temperature for which quantum effects are not pronounced,[13] to investigate simple temperature trends.

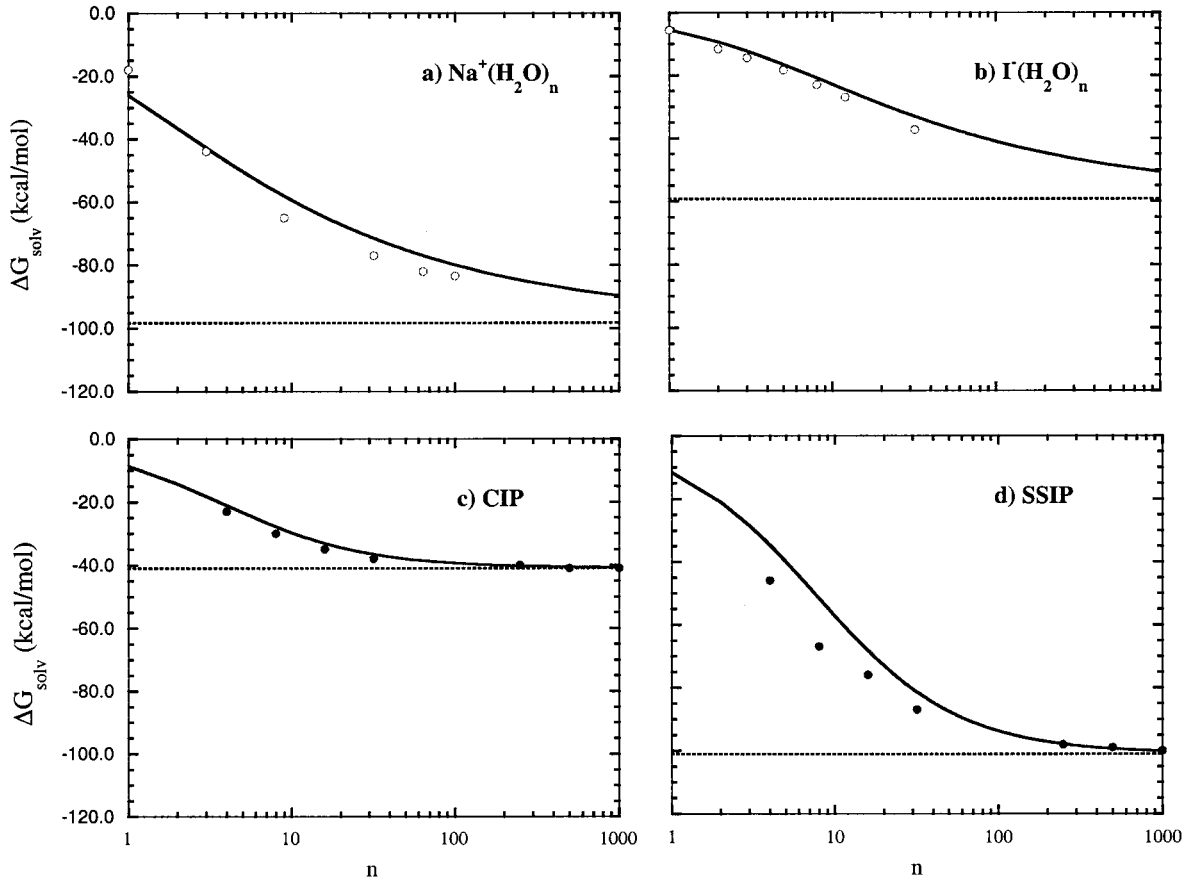

Figure 6. Solvation free energy predicted by the continuum dielectric cluster solvation model for (a) $Na^+(H_2O)_n$ clusters; (b) $I^-(H_2O)_n$ clusters; (c) CIP clusters; and (d) SSIP clusters at 300 K. The solid lines in panels (a) and (b) represent the cluster ion expression of eq 11 with ionic cavity radii for Na^+ and I^- of 1.67 and 2.77 Å, respectively [see ref 92], while the open circles (○) represent results of Monte Carlo simulations [see ref 92]. The solid lines in panels (c) and (d) represent the point−dipole expression of eqs 14 with parameters $\mu = 12.5$ D and $a = 3.0$ Å for the model CIP, and $\mu = 28.0$ D and $a = 3.8$ Å for the model SSIP, along with the results of numerical calculations (●) of the ion pair solvation free energies; the model CIP and SSIP used in the numerical calculations are described in Table 4. The dotted lines represent the respective asymptotic bulk limits. The solvent parameters for all calculations are $\epsilon = 73.15$, $\rho = 0.99224$ cm^3/mol and $M = 18.015$ g/mol [taken from ref 88c].

The potentials of mean force of the $NaI(H_2O)_n$ clusters calculated at 200 and 300 K with OPCS are compared in Figure 7, while the resulting equilibrium constants for clusters at 200 K are listed in Table 3, along with those at 300 K. A feature noticeable from the data in Figure 7 and Table 3 is that the ion pairs are even more stable with respect to dissociation as temperature is lowered. Clusters also tend to be found with more clearly defined structures, indicating a higher degree of compactness at low temperatures, as discussed elsewhere.[43] However, the CIP ⇌ SSIP equilibrium constants do not seem to exhibit a clear temperature dependence given the statistical uncertainties.

IV. Implications for $NaI(H_2O)_n$ Photodissociation Experiments

One of the main findings of this work is that the NaI ion pairs are stable with respect to complete dissociation in clusters, in contrast to the bulk solution analogue problem. This indicates in part the feasibility, for a range of cluster sizes, of the photodissociation experiments, which require stable undissociated ion pairs that possess an optically accessible excited state akin to that of isolated NaI.[30,32] We now turn our attention to the latter issue. It is plausible that a NaI "contact" ion pair surrounded by water molecules may possess an oscillator strength or transition dipole moment similar to that of the isolated NaI molecule (but of course with a different energy gap and photoexcitation wavelength). However, one may wonder about the transition dipole moment of a solvent-separated NaI ion pair, which we remind the reader is the most thermodynamically likely form of the ion pair in the larger clusters by 1 to 2 orders of magnitude compared to the CIP; cf. Table 3). While we defer the detailed study of the $NaI(H_2O)_n$ cluster absorption spectrum to a later publication, we present here several model calculations for orientation on this question.

To evaluate both ground and first electronically excited $^1\Sigma^+$ state cluster properties, we have performed model configuration interaction with single excitation [CI(S)] ab initio computations with the modified 6-31+G** basis set described in section II.B on NaI and some of the cluster structures optimized at the MP2 level of theory and shown in Figure 2.[99] The energy gap between the ground and first electronically excited $^1\Sigma^+$ states predicted by the calculations for isolated NaI at its ground state equilibrium internuclear separation is 4.7 eV, as compared to the estimated experimental isolated molecule energy gap of ∼4.2 eV, which corresponds to a typical excitation wavelength of 296 nm. Because only single excitations are considered and the basis set employed is not *very* large, these calculations are not expected to yield very accurate NaI system energetics.[99] On the other hand, our present ab initio calculations yield a ground-state dipole moment of 10.0 D at the NaI equilibrium internuclear separation which is in good agreement with both very high-level calculations[56] and experimental data (∼9.2 D).[57] Furthermore, our calculations also predict a reversed dipole moment of −5.4 D for the first excited $^1\Sigma^+$ state of NaI in the

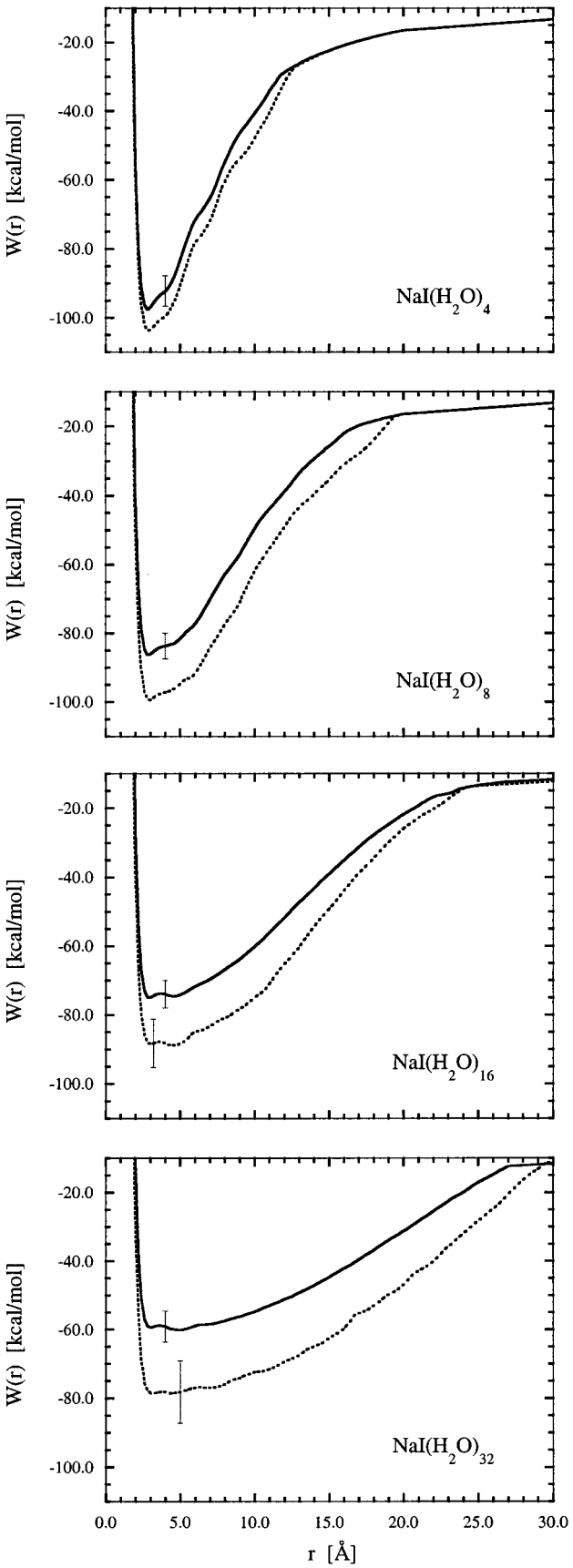

Figure 7. Comparison of the potentials of mean force computed with the OPCS model for $NaI(H_2O)_n$ clusters at 200 K (dotted line) and 300 K (solid line).

Franck−Condon region which is in excellent agreement with very high-level ab initio calculations.[56] This agreement inspires at least some confidence in the reliability of this level of theory for transition dipole moments, if not for transition oscillator strengths. In any event, we shall focus on the relative difference in NaI properties induced by the presence of solvent molecules, as predicted by the same ab initio level of theory.

TABLE 5: Properties of the First Electronically Excited $^1\Sigma^+$ $NaI(H_2O)_n$ States[a]

	ΔE^b	$\mu_{tr}{}^c$	$f_{OSC}{}^d$
NaI ($r = 2.8$ Å)	4.73	3.0	0.16
$NaI(H_2O)$ C_{2v}	5.23	2.7	0.15
$NaI(H_2O)$	5.22	2.6[e]	0.13
$NaI(H_2O)_2$	5.84	2.4	0.13
$NaI(H_2O)_3$	6.21	2.3	0.13
NaI "SSIP" ($r = 6$ Å)	1.14	4.0	0.07
$NaI(H_2O)$ "SSIP" ($r = 6$ Å)	2.79	1.9[a]	0.04

[a] CIS/6-31+G**//MP2 ab initio calculations. See text for details. [b] Energy gap with the ground $^1\Sigma^+$ state in eV. [c] Transition dipole moment in D along the bonding NaI axis. [d] Oscillator strength for an electronic transition from the ground state. [e] The transition dipole moment has a very small component orthogonal to the bonding axis (in the plane containing the water molecule).

The calculated oscillator strength for the isolated NaI transition from the ground to first excited $^1\Sigma^+$ state decreases rapidly with increasing internuclear separation, and it drops from 0.16 at $r = 2.7$ Å to 0.07 at $r = 6.0$ Å, as shown in Table 5.[100] The presence of one or more water molecules around the CIP not surprisingly increases the state energy gap (as the ground state is stabilized by the polar solvent while the first excited $^1\Sigma^+$ state, with reversed polarity, is destabilized by the solvent)[101,102] and does not significantly alter the transition dipole moment. On the other hand, Table 5 shows that the presence of a water in the middle of the ion pair causes the transition dipole moment, and the transition oscillator strength, to decrease by a factor of 2, compared to the isolated NaI case.[103] There is evidently no effective super-exchange mechanism[104] involved in the photoexcitation process.

While the above calculations remain to be performed at higher, more quantitative levels of electronic structure theory and extended to larger clusters, they suggest that, if anything, the oscillator strength for the isolated NaI transition from the ground to the first excited $^1\Sigma^+$ state at the bond extensions characteristic of the SSIP is even smaller in a cluster than for isolated NaI. There are then important implications for the possibility of photodissociation via such absorption when this feature is coupled with the results of the preceding sections, especially those of Figure 3 and Table 3 concerning the relative occurrence of CIP and SSIP configurations in clusters of increasing size. In particular, as the cluster size grows, a progressively larger fraction of the NaI ground state molecules will exist in the range of SSIP separations, with its reduced transition oscillator strength compared to that of the CIP. As a result, for sufficiently large clusters, even though the ground state ion pairs are stable with respect to complete dissociation, they will no longer be photoexcitable. While the prediction of the cluster size at which this happens is a complex calculation (also involving the effect of differing energy gaps and Franck−Condon factors),[32] the arguments above are at least consistent with the experimental observation[40,42] that laser photodissociation produces $Na^+(H_2O)_n$ cluster products of size no larger than about 50 or so, suggesting that ground state $NaI(H_2O)_n$ systems of greater than approximately this size do not absorb in the first place.[105] We add however, as a note of caution, that it may be difficult to generate large stable parent $NaI(H_2O)_n$ clusters in the experimental conditions,[40] and it is also possible that only

parent clusters of size smaller than 50 or so are generated and involved in the photodissociation experiments.

VI. Concluding Remarks

We have investigated the stability of $NaI(H_2O)_n$ cluster ion pairs by computing ion pair potentials of mean force and the resulting cluster ion pair equilibrium constants. A major finding of our theoretical study is that the ion pair is quite stable with respect to dissociation into free ions, even in very large clusters. Viewed in a larger perspective, the latter finding is in agreement with the results of NaCl simulations in supercritical water,[106,107] experimentally derived equilibrium constants for NaI (or NaCl) ion pairs in low-polarity solvents,[108,109] and recent free energy calculations of sulfuric acid ion pairs in large water mixture aerosols,[21] and obviously contrasts with the situation in aqueous solutions in ambient conditions.[45] An analysis of individual cluster ion and cluster ion pair solvation energies in terms of a simple cluster solvation dielectric model suggests that the stability of the ion pairs is in fact due to the slow convergence of the differential solvation free energy to the bulk limit, which in turn is due to the very slow convergence of cluster ion solvation energies with increasing cluster size. This makes separated cluster ions thermodynamically very unlikely, and ions rather tend to exist as "contact" or solvent-separated ion pairs. The latter species seem to become thermodynamically predominant in the larger clusters, a feature which seems nevertheless less pronounced at the low temperatures that experiments are likely to involve.

Preliminary ab initio characterization of model cluster excited states suggests that $NaI(H_2O)_n$ cluster "contact" ion pairs have optically accessible excited states akin to that of gas-phase NaI, hence making photodissociation experiments feasible. On the other hand, electronic transition oscillator strengths seem to significantly decrease for model solvent-separated ion pairs, which we remind the reader are becoming increasingly more likely with cluster size. As a result, the larger (solvent-separated) cluster ion pairs will not be involved in cluster photodissociation reactions via a mechanism akin to gas-phase NaI photodissociation, in agreement with recent experimental findings.

Even though simulations with both optimized potentials for liquid simulations (OPLS) and optimized potentials for cluster simulations (OPCS) yield results with similar conclusions, there are some notable quantitative differences in the results which can be traced back to the explicit polarization term in OPCS. For example, OPLS simulations predict an overwhelmingly stable SSIP compared to the CIP, while the ratio of ion pair populations is predicted by OPCS simulations to be about 1 to 2 orders of magnitude for the cluster sizes investigated here. This illustrates the importance of including both solute−solvent and solvent−solvent many-body polarization terms in model potentials.

Another major finding which will be reported in detail in a later publication[43] is that $NaI(H_2O)_n$ clusters tend to have surface structures,[38] due to the now well-known apparent hydrophobicity of iodide in water clusters.[6,8c,d] This may imply a slow convergence of the photodissociation dynamics of $NaI(H_2O)_n$ clusters with increasing cluster size. As clusters grow, and water molecules more likely bond to each other rather than solvate the solute, the curve crossing dynamics characteristic of NaI photodissociation might not be so dramatically affected by the presence of more water molecules: the solvent mainly affects the curve crossing dynamics by dynamically stabilizing the ion pair or the covalent NaI species, and the differential solvation energy between these states is rather insensitive to distant solvent molecules.

There may be another possible explanation for the fact that cluster products are not detected beyond size 50 or so in cluster photodissociation experiments, despite our theoretical prediction that the parent ion pair clusters are quite stable with respect to dissociation even for very large clusters (provided large stable clusters can be generated in the experiment).[40] It is possible that the photoexcitation of the larger clusters proceeds via a different route than it does for the small clusters and isolated NaI. For example, as clusters grow, the net dipole moment of the water network dramatically increases (and this feature is even more pronounced for surface clusters), and it is conceivable that the water net dipole grows large enough to dipole-bind an electron upon cluster photoexcitation, resulting in a charge-transfer-to-solvent (CTTS) excited state with totally different dynamics from that of excited-state NaI. Small clusters of iodide with water, acetone, or acetonitrile, are known to possess such CTTS excited states.[6,7] We also note that the CTTS mechanism may also be more likely for SSIPs than for CIPs, as the oscillator strength for an electronic transition to an excited state akin to that of isolated NaI is much weaker in the first place, and that SSIPs tend to exhibit more surface structures than CIPs,[43] with large net solvent dipole moments that can facilitate electron binding. Obviously, the latter excited states cannot be characterized at this stage in our model ab initio calculations, since one needs to look at rather large clusters and must employ very large, diffuse basis sets in order to describe solvated electron states.

Let us now turn our attention to other solvents for which photodissociation dynamics experiments have been performed and contrast their possible differences with water. Clusters of significantly smaller sizes have been observed experimentally for acetonitrile and ammonia than for water.[42] For the purpose of studying the ion pair clusters, their thermodynamic stability and their possible absorption, we have derived model potentials for $NaI(CH_3CN)_n$ and $NaI(NH_3)_n$ clusters and are validating these with simulations of ion−acetonitrile clusters[110] and ion−ammonia clusters.[111] Acetonitrile is a particularly interesting solvent in this context, as the CTTS mechanism mentioned above is probably more likely with only a few solvent molecules for acetonitrile, since the acetonitrile dipole is much larger than that of water and dipole-binding of an electron is thus facilitated. There is no doubt that a detailed and precise ab initio characterization of the $NaI(CH_3CN)$ excited states[112] could help explain why cluster products are detected only up to size 10 or so in $NaI(CH_3CN)_n$ cluster photodissociation experiments[40,42] if the CTTS mechanism is indeed an important factor in the process.[113] Finally, we note that, regarding the ammonia experiments, it must be much more difficult to generate large $NaI(NH_3)_n$ clusters in the first place, given the initial high temperature of the NaI vapor and the low boiling point of ammonia, and thus, the lack of large parent cluster ion pairs in the experimental cell might explain why smaller cluster products (up to size 8) are observed experimentally than for water. For example, we have found that large ion-ammonia clusters are not stable with respect to evaporation even at relatively low temperatures, and because of the very low solvent−solvent binding energies, ion−ammonia clusters with more than one solvation shell are not thermodynamically very likely.[111]

Acknowledgment. This research was supported in part by NSF grants CHE-9520619 (Colorado State University) and CHE-970049 (University of Colorado), and by a grant from the Natural Sciences and Engineering Research Council (NSERC) of Canada. J.T.H. thanks Claude Dedonder-Lardeux, Christophe Jouvet, Gilles Grégoire, and other members of the Laboratoire

de Photophysique Moléculaire (LPPM) du CNRS (UPR 3361), Université Paris-Sud, Orsay, France for many useful discussions. A portion of this work was performed while J.T.H. was, successively, an Invited Visiting Professor and a CNRS Poste Rouge Research Fellow in the LPPM in Orsay. J.T.H. also gratefully acknowledges receipt of a University of Colorado Research and Creative Work Fellowship (1997-98) in support of this work.

References and Notes

(1) See, e.g., *Chemical Reactions in Clusters*, Bernstein, E. R., Ed.; Oxford University Press: New York, 1996.

(2) See, e.g., Castleman, A. W.; Bowen, K. H. *J. Phys. Chem.* **1996**, *100*, 12911, and references therein.

(3) Kebarle, P. *Annu. Rev. Phys. Chem.* **1977**, *28*, 445.

(4) Castleman, A. W.; Keesee, R. G. *Chem. Rev.* **1986**, *86*, 589.

(5) Coe, J. V. *Chem. Phys. Lett.* **1994**, *229*, 161. Coe, J. V. *J. Phys. Chem. A* **1997**, *101*, 2055.

(6) Serxner, D.; Dessent, C. E. H.; Johnson, M. A. *J. Chem. Phys.* **1996**, *105*, 7231. Ayotte, P.; Bailey, C. G.; Weddle, G. H.; Johnson, M. A. *J. Phys. Chem. A* **1998**, *102*, 3067.

(7) Dessent, C. E. H.; Bailey, C. G.; Johnson, M. A. *J. Chem. Phys.* **1995**, *102*, 6335. Dessent, C. E. H.; Bailey, C. G.; Johnson, M. A. *J. Chem. Phys.* **1995**, *103*, 2006.

(8) (a) See, e.g., Perez, P.; Lee, W. K.; Prohofsky, E. W. *J. Chem. Phys.* **1983**, *79*, 388. Jorgensen, W. L.; Severance, D. L. *J. Chem. Phys.* **1993**, *99*, 4233. Markovich, G.; Perera, L.; Berkowitz, M. L.; Cheshnovsky, O. *J. Chem. Phys.* **1996**, *105*, 2675. Truong, T. N.; Stefanovich, E. V. *Chem. Phys.* **1997**, *218*, 31. (b) See, e.g., Sung, S.-S.; Jordan, P. C. *J. Chem. Phys.* **1986**, *85*, 4045. Lin, S.; Jordan, P. C. *J. Chem. Phys.* **1988**, *89*, 7492. (c) Perera, L.; Berkowitz, M. L. *J. Chem. Phys.* **1991**, *95*, 1954, 4236. Perera, L.; Berkowitz, M. L. *J. Chem. Phys.* **1993**, *99*, 4236. Perera, L.; Berkowitz, M. L. *J. Chem. Phys.* **1993**, *99*, 4222. Dang, L. X.; Garrett, B. C. *J. Chem. Phys.* **1993**, *99*, 2972. Dang, L. X.; Smith, D. E. *J. Chem. Phys.* **1993**, *99*, 6950. (d) Sremaniak, L. S.; Perera, L.; Berkowitz, M. L. *Chem. Phys. Lett.* **1994**, *218*, 377.

(9) See, e.g., Kistenmacher, H.; Popkie, H.; Clementi, E. *J. Chem. Phys.* **1974**, *61*, 799. Combariza, J. E.; Kestner, N. R.; Jortner, J. *Chem. Phys. Lett.* **1993**, *203*, 423. Combariza, J. E.; Kestner, N. R.; Jortner, J. *J. Chem. Phys.* **1994**, *100*, 2851.

(10) Lu, D. S.; Singer, S. J. *J. Chem. Phys.* **1996**, *105*, 3700.

(11) (a) Draves, J. A.; Luthery-Schulten, Z.; Liu, W.-L.; Lisy, J. M. *J. Chem. Phys.* **1990**, *93*, 4589. Selegue, T. J.; Moe, N.; Draves, J. A.; Lisy, J. M. *J. Chem. Phys.* **1992**, *96*, 7268. (b) Cabarcos, O. C.; Lisy, J. M. *Chem. Phys. Lett.* **1996**, *257*, 265. Weinheimer, C. J.; Lisy, J. M. *J. Phys. Chem.* **1996**, *100*, 15305.

(12) Steel, E. A.; Merz, K. M.; Selinger, A.; Castleman, A. W. *J. Phys. Chem.* **1995**, *99*, 7829.

(13) Gai, H. D.; Dang, L. X.; Schenter, G. K.; Garrett, B. C. *J. Phys. Chem.* **1995**, *99*, 13303. Gai, H. D.; Schenter, G. K.; Dang, L. X.; Garrett, B. C. *J. Chem. Phys.* **1996**, *105*, 8835.

(14) Tsai, C. J.; Jordan, K. D. *Chem. Phys. Lett.* **1993**, *213*, 181. Jensen, J. O.; Krishnan, P. N.; Burke, L. A. *Chem. Phys. Lett.* **1996**, *260*, 499.

(15) See, e.g., Liu, K.; Cruzan, J. D.; Saykally, R. J. *Science* **1996**, *271*, 929. Liu, K.; Brown, M. G.; Carter, C.; Saykally, R. J.; Gregory, J. K.; Clary, D. C. *Nature* **1996**, *381*, 501, and reference therein.

(16) Dang, L. X.; Chang, T.-M. *J. Chem. Phys.* **1997**, *106*, 8149. Dang, L. X. *J. Chem. Phys.* **1999**, *110*, 1526.

(17) Wales, D. J.; Ohmine, I. *J. Chem. Phys.* **1993**, *98*, 7245. Wales, D. J.; Ohmine, I. *J. Chem. Phys.* **1993**, *98*, 7257. Wales, D. J.; Walsh, T. R. *J. Chem. Phys.* **1996**, *105*, 6957. Wales, D. J.; Walsh, T. R. *J. Chem. Phys.* **1997**, *106*, 7193. Baba, A.; Hirata, Y.; Saito, S.; Ohmine, I.; Wales, D. J. *J. Chem. Phys.* **1997**, *106*, 3329.

(18) Hodges, M. P.; Stone, A. J.; Xantheas, S. S. *J. Phys. Chem. A* **1997**, *101*, 9163.

(19) Laria, D.; Fernandez-Prini, R. *Chem. Phys. Lett.* **1993**, *205*, 260. *J. Chem. Phys.* **1995**, *102*, 7664.

(20) Asada, T.; Nishimoto, K. *Chem. Phys. Lett.* **1995**, *232*, 518.

(21) Kusaka, I.; Wang, Z.-G.; Seinfeld, J. H. *J. Chem. Phys.* **1998**, *108*, 6829.

(22) Gertner, B. J.; Peslherbe, G. H.; Hynes, J. T. *Isr. J. Chem.* **2000**, *39*, 273.

(23) Tucker, S. C.; Truhlar, D. G. *J. Am. Chem. Soc.* **1990**, *112*, 3347.

(24) See, e.g., Wilse Robinson, G.; Zhu, S.-B.; Singh, S.; Evans, M. W. *Water in Biology, Chemistry and Physics: Experimental Overview and Computational Methodologies*, World Scientific: Singapore, 1996.

(25) Mason, B. J. *The Physics of Clouds*, 2nd ed.; Oxford University Press: London, 1971. Byers, H. R. *Elements of Cloud Physics*; University of Chicago Press: Chicago & London, 1965.

(26) Fletcher, N. H. *The Physics of Rainclouds*; University Press: Cambridge, 1962.

(27) Battan, L. J. *Cloud Physics and Cloud Seeding*; Doubleday: Garden City, NY, 1962.

(28) Beichert, P.; Finlayson-Pitts, B. J. *J. Phys. Chem.* **1996**, *100*, 15218. Langer, S.; Pemberton, R. S.; Finlayson-Pitts, B. J. *J. Phys. Chem. A* **1997**, *101*, 1277. DeHaan, D. O.; Finlayson-Pitts, B. J. *J. Phys. Chem. A* **1997**, *101*, 9993. Oum, K. W.; Lakin, M. J.; DeHaan, D. O.; Brauer, T.; Finlayson-Pitts, B. J. *Science* **1998**, *279*, 74.

(29) George, C.; Ponche, J. L.; Mirabel, P.; Behnke, W.; Scheer, V.; Zetzsch, C. *J. Phys. Chem.* **1994**, *98*, 8780. George, C.; Behnke, W.; Scheer, V.; Zetzsch, C.; Magi, L.; Ponche, J. L.; Mirabel, P. *Geophys. Res. Lett.* **1995**, *22*, 1505. Schweitzer, F.; Magi, L.; Mirabel, P.; George, C. *J. Phys. Chem. A* **1998**, *102*, 593.

(30) Rosker, M. J.; Rose, T. S.; Zewail, A. H. *Chem. Phys. Lett.* **1988**, *146*, 175. Rose, T. S.; Rosker, M. J.; Zewail, A. H. *J. Chem. Phys.* **1988**, *88*, 6672. Rose, T. S.; Rosker, M. J.; Zewail, A. H. *J. Chem. Phys.* **1989**, *91*, 7415. Zewail, A. H. *J. Chem. Soc., Faraday Trans.* **1989**, *85*, 1221. Cong, P.; Mohktari, A.; Zewail, A. H. *Chem. Phys. Lett.* **1990**, *172*, 109. Mohktari, A.; Cong, P.; Herek, J. L.; Zewail, A. H. *Nature* **1990**, *348*, 225. Zewail, A. H. *Faraday Trans. Chem. Soc.* **1991**, *91*, 207. Zewail, A. H. *Femtochemistry − Ultrafast Dynamics of the Chemical Bond*; World Scientific: Singapore, 1994. Zewail, A. H. In *Femtosecond Chemistry*; Manz J.; Wöste L., Eds.; VCH: New York, 1994; Vol. 1, p 15. Cong, P.; Roberts, G.; Herek, J. L.; Mohktari, A.; Zewail, A. H. *J. Chem. Phys.* **1996**, *100*, 7832.

(31) Lin, S. H.; Fain, B.; Hamer, N. In *Advances in Chemical Physics*; Prigogine, I., Rice, S. A., Eds.; Wiley: New York, 1990; Vol. 74; p 123.

(32) Jouvet, C.; Martrenchard, S.; Solgadi, D.; Dedonder-Lardeux, C.; Mons, M.; Grégoire, G.; Dimicoli, I.; Piuzzi, F.; Visticot, J. P.; Mestdagh, J. M.; Doliveira, P.; Meynadier, P.; Perdrix, M. *J. Phys. Chem.* **1997**, *101*, 2555. Grégoire, G.; Mons, M.; Dimicoli, I.; Piuzzi, F.; Charron, E.; Dedonder-Lardeux, C.; Jouvet, C.; Martrenchard, S.; Solgadi, D.; Suzor-Weiner, A. *Eur. Phys. J. D* **1998**, *1*, 187.

(33) Lee, S.-Y.; Pollard, W. T.; Mathies, R. A. *J. Chem. Phys.* **1989**, *90*, 6146.

(34) Engel, V.; Metiu, H.; Almeida, R.; Marcus, R. A.; Zewail, A. H. *Chem. Phys. Lett.* **1988**, *152*, 1. Engel, V.; Metiu, H. *J. Chem. Phys.* **1989**, *90*, 6116.

(35) Engel, V.; Metiu, H. *Chem. Phys. Lett.* **1989**, *155*, 77. Braun, M.; Meier, C.; Engel, V. *J. Chem. Phys.* **1996**, *105*, 530.

(36) Martinez, T. J.; Levine, R. D. *Chem. Phys. Lett.* **1996**, *259*, 252. Martinez, T. J.; Levine, R. D. *J. Chem. Phys.* **1996**, *105*, 6334.

(37) Peslherbe, G. H.; Bianco, R.; Hynes, J. T.; Ladanyi, B. M. *J. Chem. Soc., Faraday Trans.* **1997**, *93*, 977.

(38) Peslherbe, G. H.; Ladanyi, B. M.; Hynes, J. T. *J. Phys. Chem. A* **1998**, *102*, 4100.

(39) Peslherbe, G. H.; Ladanyi, B. M.; Hynes, J. T. Nonadiabatic Trajectory Studies of the Photodissociation Dynamics of NaI in Small Water Clusters, manuscript in preparation.

(40) Jouvet, C.; Dedonder-Lardeux, C., private communication.

(41) *CRC Handbook of Chemistry and Physics*, 77th ed.; Lide, D. R., Ed.; CRC: Boca Raton, FL, 1996.

(42) Grégoire, G.; Mons, M.; Dedonder-Lardeux, C.; Jouvet, C. *Eur. Phys. J. D* **1998**, *1*, 5. Grégoire, G.; Mons, M.; Dimicoli, I.; Dedonder-Lardeux, C.; Jouvet, C.; Martrenchard, S.; Solgadi, D. *J. Chem. Phys.* **1999**, *110*, 1521.

(43) Peslherbe, G. H.; Ladanyi, B. M.; Hynes, J. T. Structure of NaI Ion Pairs in Water Clusters *Chem. Phys.*, Special Issue on water, in press.

(44) See, e.g., Hill, T. L. *Statistical Mechanics. Principles and Selected Applications*, McGraw-Hill: New York, 1956; p. 193. Davidson, N. *Statistical Mechanics*, McGraw-Hill: New York, 1962; p. 481.

(45) Guàrdia, E.; Rey, R.; Padró, J. A. *Chem. Phys.* **1991**, *155*, 187. Dang, L. X. *J. Chem. Phys.* **1992**, *97*, 1919.

(46) Valleau, J.; Patey, G. N. *J. Chem. Phys.* **1975**, *63*, 2334. Berkowitz, M.; Karim, O. A.; McCammon, J. A.; Rossky, P. J. *Chem. Phys. Lett.* **1984**, *105*, 577. Karim, O. A.; McCammon, J. A. *J. Am. Chem. Soc.* **1986**, *108*, 1762. Dang, L. X.; Pettit, B. M. *J. Chem. Phys.* **1987**, *86*, 6560. Buckner, J. K.; Jorgensen, W. L.; Houston, S. E.; Rossky, P. J. *J. Am. Chem. Soc.* **1987**, *109*, 1981. Buckner, J. K.; Jorgensen, W. L. *J. Am. Chem. Soc.* **1989**, *111*, 2507. Guàrdia, E.; Rey, R.; Padró, J. A. *J. Chem. Phys.* **1991**, *95*, 2823. Zhu, S.-B.; Robinson, G. W. *J. Chem. Phys.* **1992**, *97*, 4336.

(47) Ciccotti, G.; Ferrario, M.; Hynes, J. T.; Kapral, R. *Chem. Phys.* **1989**, *129*, 241.

(48) Jorgensen, W. L.; Chandrasekhar, J.; Madura, J. D.; Impey, R. W.; Klein, M. L. *J. Chem. Phys.* **1983**, *79*, 926.

(49) Chandrasekhar, J.; Spellmeyer, D. C.; Jorgensen, W. L. *J. Am. Chem. Soc.* **1984**, *106*, 903.

(50) Allen, M. P.; Tildesley, D. J. *Computer Simulation of Liquids*; Oxford University Press: New York, 1989.

(51) Jorgensen, W. L.; Tirado-Rives, J. *J. Phys. Chem.* **1996**, *100*, 14508.

(52) It should be pointed out that computer simulations are performed for isolated clusters, whereas actual experimental measurements involve

clusters of various size in thermodynamic equilibrium with the solvent vapor. The proper definition of the physical cluster has been a long-standing issue in investigations of nucleation and capillarity phenomena, but it is now generally agreed that thermodynamic properties computed for isolated clusters, the only practical approach at this point, give an adequate representation of the properties of clusters in equilibrium with the solvent vapor under realistic experimental conditions. See. e.g., Seinfeld, J. H.; Pandis, S. N. *Atmospheric Chemistry and Physics: From Air Pollution to Climate Change*, Wiley: New York, 1998; p. 569. Lee, J. K.; Barker, J. A.; Abraham, F. F. *J. Chem. Phys.* **1973**, *58*, 3166. Reiss, H.; Tabazadeh, A.; Talbot, J. *J. Chem. Phys.* **1990**, *92*, 1266. Weakliem, C. L.; Reiss, H. *J. Phys. Chem.* **1994**, *98*, 6408.

(53) Lu, D. S.; Singer, S. J. *J. Chem. Phys.* **1995**, *103*, 1913.

(54) Asher, R. L.; Micha, D. A.; Brucat, P. J. *J. Chem. Phys.* **1992**, *96*, 7683.

(55) Mulliken, R. S. *J. Chim. Phys.* **1949**, *46*, 497. Pariser, R. *J. Chem. Phys.* **1953**, *21*, 568. Pohl, H. A.; Rein, R.; Appel, K. *J. Chem. Phys.* **1964**, *41*, 3383.

(56) Sakai, Y.; Miyoshi, E.; Anno, T. *Can. J. Chem.* **1992**, *70*, 309.

(57) Hebert, A. J.; Lovas, F. J.; Melenders, C. A.; Hollowell, C. D.; Story, T. L.; Street, K. *J. Chem. Phys.* **1968**, *48*, 2834.

(58) Karplus, M.; Porter, R. N. *Atoms and Molecules; an Introduction for Students of Physical Chemistry*; W. A. Benjamin: New York, 1970.

(59) Peslherbe, G. H.; Koch, D.; Ladanyi, B. M.; Hynes, J. T. A Molecular Dynamics Study of Water Clusters and Liquid Water with a New Simple Polarizable Water Model, manuscript in preparation.

(60) Wallqvist, A.; Ahlstrom, P.; Karlstrom, G. *J. Phys. Chem.* **1990**, *94*, 1649.

(61) In the NEMO model of ref 60, individual contributions (electrostatic, polarization, dispersion, etc.) to the solvent−solvent binding energy are arbitrarily obtained from ab initio data and used as the basis for parameterization.

(62) The importance of the water model quadrupole moments has also been strongly implicated in the adequate description of bulk liquid properties [Carnie, S. L.; Patey, G. N. *Mol. Phys.* **1982**, *47*, 1129. See also ref 64].

(63) Even though they were not explicitly included in the parameterization procedure, the octupole moments of our water model point charge distribution are also in semiquantitative agreement with the predictions of ab initio calculations (see ref 59).

(64) Chialvo, A. A.; Cummings, P. T. *J. Chem. Phys.* **1996**, *105*, 8274.

(65) Perera, L.; Amar, F. G. *J. Chem. Phys.* **1989**, *90*, 7354.

(66) Press, W. H.; Teukolsky, S. A.; Vetterling, W. T.; Flannery, B. P. *Numerical Recipes, the Art of Scientific Computing*, 2nd ed.; Cambridge University Press: Cambridge, England, 1992.

(67) Tessman, J. R.; Kahn, A. H.; Shockley, W. *Phys. Rev.* **1953**, *92*, 890.

(68) Another approach for introducing polarization effects in molecular systems is the electronegativity equalization [Mortier, W. J.; Ghosh, S. K.; Shankar, S. *J. Am. Chem. Soc.* **1986**, *108*, 4315. York, D. M. *Int. J. Quantum Chem., Quantum Chem. Symp.* **1995**, *29*, 385] or charge equilibration method of Rappé et al. [Rappé, A. K.; Goddard, W. A. *J. Phys. Chem.* **1991**, *95*, 3358], which can be derived from density functional theory [Parr, R. G.; Yang, W. *Density-Functional Theory of Atoms and Molecules*, Clarendon Press: New York, 1989]. Briefly, in this method, the atomic charges are solved by minimizing the total electrostatic energy of the molecular system (or equivalently equating the atomic chemical potentials), and the atomic energy is usually assumed to be a parameterized quadratic form of the atomic charges. The charge equilibration method has had success describing the charge distributions of large molecules at their ground state equilibrium geometry, and fluctuating charge water models employing this technique have been proposed, such as the TIP4P−FQ model of Berne and co-workers [Rick, S. W.; Stuart, S. J.; Berne, B. J. *J. Chem. Phys.* **1994**, *101*, 6141. Rick, S. W.; Stuart, S. J.; Bader, J. S.; Berne, B. J. *J. Mol. Liq.* **1995**, *65/66*, 31], which reproduces various properties of liquid water quite well. However, we were unable to reproduce both the energetics and (ab initio) charge distribution of ion−water clusters or ion pair−water clusters, whether we employed the TIP4P−FQ and OPLS parameters, the original parameters of Rappé et al., or a combination of both sets. Another set of more adequate parameters could be derived, but they did not seem to be appropriate for describing the ion pair−water cluster charge distribution over a wide range of NaI internuclear separations. Thus, it appears that the quadratic expression in the atomic charges assumed for the atomic energy may not be a very good representation of the polarization energy for the complex molecular systems studied here, and the method does not seem readily applicable to chemical systems that react or dissociate. The Rappé group is presently developing extensions of the charge equilibration method to reacting systems (A. K. Rappé, private communication).

(69) Schmidt, M. W.; Baldridge, K. K.; Boatz, J. A.; Elbert, S. T.; Gordon, M. S.; Jensen, J. J.; Koseki, S.; Matsunaga, N.; Nguyen, K. A.; Su, S.; Windus, T. L.; Dupuis, M.; Montgomery, J. A. *J. Comput. Chem.* **1993**, *14*, 1347.

(70) *Gaussian 98* (Revision A.1), Frisch, M. J.; Trucks, G. W.; Schlegel, H. B.; Scuseria, G. E.; Robb, M. A.; Cheeseman, J. R.; Zakrzewski, V. G.; Montgomery, J. A.; Stratmann, R. E.; Burant, J. C.; Dapprich, S.; Millam, J. M.; Daniels, A. D.; Kudin, K. N.; Strain, M. C.; Farkas, O.; Tomasi, J.; Barone, V.; Cossi, M.; Cammi, R.; Mennucci, B.; Pomelli, C.; Adamo, C.; Clifford, S.; Ochterski, J.; Petersson, G. A.; Ayala, P. Y.; Cui, Q.; Morokuma, K.; Malick, D. K.; Rabuck, A. D.; Raghavachari, K.; Foresman, J. B.; Cioslowski, J.; Ortiz, J. V.; Stefanov, B. B.; Liu, G.; Liashenko, A.; Piskorz, P.; Komaromi, I.; Gomperts, R.; Martin, R. L.; Fox, D. J.; Keith, T.; Al-Laham, M. A.; Peng, C. Y.; Nanayakkara, A.; Gonzalez, C.; Challacombe, M.; Gill, P. M. W.; Johnson, B. G.; Chen, W.; Wong, M. W.; Andres, J. L.; Head-Gordon, M.; Replogle, E. S.; Pople, J. A. Gaussian, Inc.: Pittsburgh, PA, 1998.

(71) Levine, I. N. *Quantum Chemistry*, 4th ed.; Prentice Hall: Englewood Cliffs, NJ, 1991.

(72) Ditchfield, R.; Hehre, W. J.; Pople, J. A. *J. Chem. Phys.* **1971**, *54*, 724. Hehre, W. J.; Ditchfield, R.; Pople, J. A. *J. Chem. Phys.* **1972**, *56*, 2257. Francl, M. M.; Pietro, W. J.; Hehre, W. J.; Binkley, J. S.; Gordon, M. S.; DeFrees, D. J.; Pople, J. A. *J. Chem. Phys.* **1982**, *77*, 3654. Hariharan, P. C.; Pople, J. A. *Theor. Chim. Acta* **1973**, *28*, 213−222.

(73) Stevens, W. J.; Basch, H.; Krauss, M. *J. Chem. Phys.* **1984**, *81*, 6026. Stevens, W. J.; Basch, H.; Krauss, M.; Jasien, P. *Can. J. Chem.* **1992**, *70*, 612. Cundari, T. R.; Stevens, W. J. *J. Chem. Phys.* **1993**, *98*, 5555.

(74) Frisch, M. J.; Pople, J. A.; Binkley, J. S. *J. Chem. Phys.* **1984**, *80*, 3265.

(75) VanDuijneveldt-VanDeRijdt, J. G. C. M.; VanDuijneveldt, F. B. *J. Mol. Struct. 89*, 185.

(76) Boys, S. F.; Bernardi, F. *Mol. Phys.* **1970**, *19*, 553.

(77) Singh, U. C.; Kollman, P. A. *J. Comput. Chem.* **1984**, *5*, 129.

(78) See, e.g., Pettitt, B. M.; Rossky, P. J. *J. Chem. Phys.* **1986**, *84*, 5836.

(79) See, e.g., Buckner, J. K.; Jorgensen, W. L. *J. Am. Chem. Soc.* **1989**, *111*, 2507.

(80) Bennett, C. H. *J. Comput. Phys.* **1976**, *22*, 245.

(81) Jorgensen, W. L.; Blake, J. F.; Buckner, J. K. *Chem. Phys.* **1989**, *129*, 193.

(82) Prue, J. E. *J. Chem. Educ.* **1969**, *46*, 13. Justice, M.-C.; Justice, J.-C. *J. Sol. Chem.* **1976**, *5*, 543.

(83) The "free" ion concentrations are defined in terms of the Na^+ and I^- solvated in separate clusters, with $W(r)$ defined to be zero in this situation, thereby defined as an asymptotic reference free energy.

(84) The convergence referred to is "local", in that contributions from more than a few kT units above the SSIP minimum are negligible, so long as one restricts the integration to the neighborhood of the SSIP well.

(85) The CIP cluster diameter is simply estimated as the largest intermolecular O−H distance in the cluster structure, and the average cluster dimension is found by averaging over a few thousands cluster configurations. Since the upper bound of the SSIP integral is in practice always smaller than the CIP cluster diameter, the SSIP population integral obviously does not include configurations corresponding to "free" ions solvated in separate clusters.

(86) Simulations of NaI in liquid water, with the same model potentials as employed here, are underway to make a more quantitative comparison between clusters and bulk solution results. Peslherbe, G. H.; Koch, D., unpublished results.

(87) The polarization of the water molecule does not depend on its local environment and is only represented in an average way with the TIP4P model. The dipole moment of the TIP4P water is close to that of liquid water.

(88) (a) Lee, N.; Keesee, R. G.; Castleman, A. W. *J. Colloid Interface Sci.* **1980**, *75*, 555. (b) Thomson, J. J. *Application of Dynamics to Physics and Chemistry*, 1st ed.; Cambridge University Press: Cambridge, 1888. (c) Holland, P. M.; Castleman, A. W. *J. Phys. Chem.* **1982**, *86*, 4181.

(89) Castleman, A. W.; Holland, P. M.; Keesee, R. G. *J. Phys. Chem.* **1978**, *68*, 1760.

(90) Jortner, J. *Mol. Phys.* **1962**, *5*, 257. Barnett, R. N.; Landman, U.; Cleveland, C. L.; Jortner, J. *Chem. Phys. Lett.* **1988**, *145*, 382.

(91) Barnett, R. N.; Landman, U.; Cleveland, C. L.; Jortner, J. *J. Chem. Phys.* **1988**, *88*, 4429. Rips, I.; Jortner, J. *J. Chem. Phys.* **1992**, *97*, 536.

(92) Peslherbe, G. H.; Ladanyi, B. M.; Hynes, J. T. *J. Phys. Chem. A* **1999**, *103*, 2561.

(93) Ghio, C.; Scrocco, E.; Tomasi, J. In *Environmental Effects on Molecular Structures and Properties*; B. Pullman, Ed.; Reidel: Dordrecht, 1976. Miertus, S.; Scrocco, E.; Tomasi, J. *Chem. Phys.* **1981**, *55*, 117. Pascual-Ahuir, J. L.; Silla, E.; Tomasi, J.; Bonaccorsi, R. *J. Comput. Chem.* **1987**, *8*, 778.

(94) The method actually proves exact for point charges.

(95) Böttcher, C. J. F. *Theory of Electric Polarization*, 2nd ed.; Elsevier: Amsterdam, 1973.

(96) Equation 13 makes the assumption that, within the cluster, the electric field **E** can be approximated by that [see ref 95] of a point dipole in a bulk dielectric continuum. An alternate route for ΔG_{solv} is to solve the Poisson equation exactly [see ref 95] for a point dipole, and this yields $\Delta G_{solv} = -\mu^2/a^3(\epsilon - 1)/(2\epsilon + 1)\ 1 - f(R)]$, where $f(R) = 9\epsilon/[(2\epsilon + 1)(\epsilon + 2)(R/a)^3 - 2(\epsilon - 1)^2]$, which also predicts a rapid convergence (as

R^{-3}) to the bulk limit. We have not followed other possible routes [see, e.g., Dilonardo, M.; Maestro, M. *Chem. Phys. Lett.* **1991**, *180*, 353] either, since (a) the major purpose is to demonstrate the rapid R^{-3} convergence and (b) the approximation in eq 13 is most similar to that made in the numerical model calculations to which it is compared in Figure 6.

(97) The evaporative ensemble model has been discussed and/or reviewed in: Klots, C. E. *Nature* **1987**, *327*, 222. Klots, C. E. *Int. J. Mass Spectrom. Ion Processes* **1990**, *100*, 457. Klots, C. E. *Z. Phys. D* **1991**, *20*, 105. Klots, C. E. *Z. Phys. D* **1991**, *21*, 335. Klots, C. E. *J. Chem. Phys.* **1993**, *98*, 1110.

(98) The impact of temperature and quantum effects on the $NaI(H_2O)_n$ cluster thermodynamics is being studied in greater detail using quantum Monte Carlo simulations. Peslherbe, G. H.; Faivre, D. unpublished results.

(99) In contrast to the MP2 calculations discussed in section II.B.3, which are nonvariational but presumably yield reliable relative energies, CI(S) calculations are not *size-consistent*; this means that this level of theory is certainly insufficient to describe the NaI ground and first electronically excited state energy curves over the whole range of NaI internuclear separations. Using a not *very* large basis set like the modified 6-31+G** decreases the size-consistency error (and the small correlation space in CI-(S) calculations presumably decreases the basis-set-superposition-error), but also results in a poorer description of the wave function in general. CI calculations can be made size-consistent at the expense of including up to quadrupole excitations, but reliable CI calculations require *very* large basis sets in any event [see, e.g., ref 71]. It should also be noted that a rigorous treatment of the NaI system should include spin−orbit coupling [see refs 36 and 56], which splits the energy levels of atomic iodine by as much as 0.96 eV [see Moore, C. E. *Atomic Energy Levels*; U.S. GPO: Washington, 1958], and certainly must be significant for NaI as well.

(100) Note that a more refined treatment such as a multireference CI is more justified for model SSIPs than for CIPs, since the NaI wave function at large internuclear separations is best represented as a combination of ionic and covalent references, especially close to the avoided crossing region. As a result, the present CI(S) results may be more reliable for model CIPs than for SSIPs.

(101) Note that the increase in the state energy gap of the ion pair clusters is consistent with the ion pair solvation energies (i.e., the cluster binding energies) calculated with the MP2 level of theory and listed in Table 2.

(102) We anticipate that the blue shifting evident in Table 5 for increasing number of solvent molecules would cease with several solvent shells.

(103) It is important to note that the results quoted for 6 Å separations are at separations for which a SSIP is only stable for larger clusters (cf. Table 3); there are no stable SSIP species at this separation for the clusters in Table 5. This however does not compromise the point of Table 5, which is to indicate trends in energy gap, transition dipole moment and oscillator strength for the ion pair upon addition of water solvent molecules.

(104) Liang, C.; Newton, M. D. *J. Phys. Chem.* **1993**, *97*, 3199. Cave, R. J.; Newton, M. D.; Kumar, K.; Zimmt, M. B. *J. Phys. Chem.* **1995**, *99*, 17501.

(105) This aspect was first clarified in discussions of C. Jouvet (Orsay) and J.T.H.

(106) Gao, J. L. *J. Phys. Chem.* **1994**, *98*, 6049.

(107) Chialvo, A. A.; Cummings, P. T.; Simonson, J. M.; Mesmer, R. E. *J. Mol. Liq.* **1997**, *73*−*74*, 361.

(108) Piekarski, H.; Tkaczyk, M.; Bald, M.; Szejgis, A. *J. Mol. Liq.* **1997**, *73*−*74*, 209.

(109) Fawcett, W. R.; Tikanen, A. C. *J. Mol. Liq.* **1997**, *73*−*74*, 373.

(110) Peslherbe, G. H.; Nguyen, T. N., work in progress.

(111) Peslherbe, G. H.; Harpham, M. R.; Ladanyi, B. M.; Hynes, J. T., work in progress.

(112) Peslherbe, G. H., unpublished results.

(113) A recent theoretical study [Grégoire, G.; Brenner, V.; Millié, P. "Energetic and Structures of $NaI(CH_3CN)_{n=1,9}$ Clusters: A Theoretical Study of the Contact Ion Pair Versus the Separated Ion Pair Structures in a Molecular Cluster", submitted to *J. Phys. Chem. A*] suggests that at 0 K the SSIP is the most energetically stable structure for clusters as small as $n = 9$. On the other hand, we have performed preliminary simulations which indicate that $NaI(CH_3CN)_n$ ($n = 12$) may exist preferentially as CIPs *at room temperature*. In light of our present findings for water, these clusters might thus have optically accessible excited states and could be involved in the cluster photodissociation experiments unless some alternative CTTS mechanism is involved. These issues deserve further investigation.